

**SUPPRESSION OF COFFEE-RING EFFECT IN RANDOM  
OPTICAL POTENTIALS**

A THESIS SUBMITTED TO  
THE GRADUATE SCHOOL OF NATURAL AND APPLIED SCIENCES  
OF  
MIDDLE EAST TECHNICAL UNIVERSITY

MERVE YAĞMUR YARDIMCI

IN PARTIAL FULFILLMENT OF THE REQUIREMENTS  
FOR  
THE DEGREE OF MASTER OF SCIENCE  
IN  
PHYSICS

AUGUST 2017



Approval of the thesis:

**SUPPRESSION OF COFFEE-RING EFFECT IN RANDOM  
OPTICAL POTENTIALS**

submitted by **MERVE YAĞMUR YARDIMCI** in partial fulfillment of the requirements for the degree of **Master of Science in Physics Department, Middle East Technical University** by,

Prof. Dr. Gülbin Dural Ünver \_\_\_\_\_  
Dean, Graduate School of **Natural and Applied Sciences**

Prof. Dr. Altuğ Özpineci \_\_\_\_\_  
Head of Department, **Physics**

Assoc. Prof. Dr. Alpan Bek \_\_\_\_\_  
Supervisor, **Physics Department, METU**

**Examining Committee Members:**

Assoc. Prof. Dr. Filiz Korkmaz Özkan \_\_\_\_\_  
Electrical and Electronics Engineering Dep, Atılım Uni.

Assoc. Prof. Dr. Alpan Bek \_\_\_\_\_  
Physics Department, METU

Assoc. Prof. Dr. Hande Toffoli \_\_\_\_\_  
Physics Department, METU

Assoc. Prof. Dr. Serhat Çakır \_\_\_\_\_  
Physics Department, METU

Assist. Prof. Dr. Emre Yüce \_\_\_\_\_  
Physics Department, METU

**Date:** \_\_\_\_\_

I hereby declare that all information in this document has been obtained and presented in accordance with academic rules and ethical conduct. I also declare that, as required by these rules and conduct, I have fully cited and referenced all material and results that are not original to this work.

Name, Last Name: MERVE YAĞMUR YARDIMCI

Signature :

# ABSTRACT

## SUPPRESSION OF COFFEE-RING EFFECT IN RANDOM OPTICAL POTENTIALS

Yardımcı, Merve Yağmur

M.S., Department of Physics

Supervisor : Assoc. Prof. Dr. Alpan Bek

August 2017, 73 pages

Drying a liquid (e.g. water) drop containing uniformly dispersed microscopic particles results in the particles' migration towards the edges of the drop; after the drop evaporates the suspended particles remain concentrated around the original drop edge. This so-called "coffee-ring" effect does not depend on the nature of the solvent or the solute; thus it is ubiquitous in nature and challenging to avoid. However, in many applications such as inkjet printing, coating and many other biological processes, there is need to suppress and control the coffee-ring effect due to the requirement of uniform deposition of the suspended particles. Such approaches include changing the shape of the particulate suspension, using acoustic waves, or adding hydrosoluble polymer during the evaporation. In this work, we investigate the evaporation of liquid droplets containing passive and active particles under random optical potentials. In particular, we experimentally show that while drops of a suspension of  $3\text{-}\mu\text{m}$  diameter polystyrene particles show typical coffee-ring when no optical potentials are applied, they

form uniform distribution, suppressing the coffee-ring formation when a random optical potential is present.

Keywords: Self-assembled patterns, evaporating droplets, bacteria, optical trapping, speckle pattern

# ÖZ

## OPTİK POTANSİYEL ALTINDA KAHVE HALKASI ETKİSİNİN BASTIRILMASI

Yardımcı, Merve Yağmur  
Yüksek Lisans, Fizik Bölümü  
Tez Yöneticisi : Doç. Dr. Alpan Bek

Ağustos 2017 , 73 sayfa

Homojen şekilde dağılmış mikroskobik parçacıkları içeren bir sıvı damlasının (örneğin su) kurumaması, damlanın kenarlarına doğru oluşan parçacık göçü ile sonuçlanır. Damla kuruduktan sonra, akışkan içerisinde asılı kalmış olan parçacıklar esas damlanın kenarında konsantre bir şekilde kalırlar. Doğada her yerde karşılaşmamızın mümkün olduğu ve kaçınılması güç olan, “kahve halkası” etkisi olarak bilinen bu durum çözücü veya çözünmüş maddenin doğasına bağlı değildir. Bununla birlikte; mürekkep püskürtmeli baskı, kaplama ve çeşitli biyolojik işlemler gibi sayısız birçok uygulamada, asılı parçacıkların homojen çökmesi gereksiniminden dolayı, “kahve halkası” etkisini bastırma ve kontrol altına alma ihtiyacı duyulmaktadır. Askıda kalan parçacık şeklinin değiştirilmesi, akustik dalgaların kullanılması, veya buharlaşma esnasında suda çözülebilen polimer ilave edilmesi bu amaca yönelik kullanılabilecek yöntemlerden birkaçıdır. Bu çalışmada ise, optik potansiyel uygulandığı takdirde kahve halkası etkisinin nasıl bir değişime

uğrayacağı gözlemlenmek istenmiştir. Aktif ve pasif parçacıklar içeren sıvı damlacıkların gelişigüzel optik potansiyelleri altındaki buharlaşması araştırılmıştır. Özellikle, 3 mikrometre çapındaki polystyrene parçacıklarından oluşan damlalar kururken optik potansiyelin olmaması durumunda tipik kahve halkası etkisi gösterirken, optik potansiyel uygulandığında parçacıkların homojen bir dağılım gösterdiğini deneysel olarak göstermiş bulunmaktayız.

Anahtar Kelimeler: Kendiliğinden oluşan desenler, buharlaşan damlalar, bakteri, optik tuzaklama, benek deseni

*To my beloved family*

## ACKNOWLEDGMENTS

First of all, I would like to express my sincere appreciation and gratitude to my supervisor dear Assoc. Prof. Dr. Alpan Bek for his invaluable supervision, kind support, and continuous guidance in preparation of this thesis. It was a great honor to work with him for the last six years, including my undergraduate and graduate life, and our cooperation influenced my academical and world view highly. Thanks to his worldview, perspective on life and his positive attitudes, he has contributed to me in many different ways, not just in my academic work. I will always be grateful to him..

The second most important person that I would like to express my special thanks to is Dr. Sabareesh K. P. Velu for his valuable contributions, enlightening guidance, kind supervision and encouraging attitude during the preparation of this study. His ideas and support made it possible that in a short time I were able to build the frame of this work and progress it. I would also like to thank his wife Kalaivani Thangavel and their little angle Anisha for their continuous smiling face, friendliness, support and sincerity.

I would also like to thank to dear Assoc. Prof. Dr. Giovanni Volpe, who is the group leader of Soft Matter Group at Advanced Research Laboratories at Bilkent University, for providing me laboratory and equipment facilities that I utilized during my thesis studies.

This work is also supported by TÜBİTAK-BİDEB MSc scholarship (2210) and TÜBİTAK-ARDEB Scientific and Technological Research Project Program (1001) (Project No: 115M061, Project Title: Development of High Efficiency Thin Film Crystal Si Solar Cell by Laser Crystallization Method).

And there are a lot of people that were with me in this process. It is not possible to write down why each of them is important to me and this work, because it will take more space than the work itself. So I'll just give names of some of them; İrem Yılmaz, Tuğba Andaç, Murad Ramanovski, Yasin Karabiber, Mahsa Seyed-mohammadzadeh, Başak Renkliođlu, Yelda Kadiođlu, Alireza Moradi, Naveed Mahmood, Breera Mahmood, Sedanur Toraman, Gözdenur Toraman, İpek Kamoy, Suat Ođur..

And finally, I feel grateful to my family and I want to dedicate this thesis to my family. Most of all, I would like to express my sincere gratitude to my mother İlfer Yardımcı, my father Erol Engin Yardımcı and my brother Ahmet Güneş Yardımcı for their enduring love, unconditional support and encouragement, which have been the real inspiration during my studies. They defined me, they made me who I am, so they are true owners of this work. Without their help and beliefs to me, I could not be the person I am right now..

# TABLE OF CONTENTS

ABSTRACT . . . . .	v
ÖZ . . . . .	vii
ACKNOWLEDGMENTS . . . . .	x
TABLE OF CONTENTS . . . . .	xii
LIST OF TABLES . . . . .	xv
LIST OF FIGURES . . . . .	xvi
CHAPTERS	
1 INTRODUCTION . . . . .	1
2 CONDENSED MATTER PHYSICS . . . . .	7
2.1 Hard Condensed Matter . . . . .	8
2.2 Soft Condensed Matter . . . . .	9
2.2.0.1 Active and Passive Soft Matter . . . . .	9
2.3 What makes colloidal particles so special? . . . . .	11
2.3.1 Properties of Colloidal Dispersions . . . . .	12
2.3.1.1 Optical Property: Tyndall Effect . . . . .	13
2.3.1.2 Kinetic Property: Brownian Motion . . . . .	14

	2.3.1.3	Electrical Properties . . . . .	15
	2.3.2	Applications . . . . .	16
3		OPTICAL TRAPPING . . . . .	19
	3.1	Introduction . . . . .	19
	3.2	The Physics behind the Optical Trapping . . . . .	20
	3.2.1	The forces generated by optical tweezers . . . . .	21
		3.2.1.1 Ray Optics Approximation ( $d \gg \lambda$ ) (Mie-Regime) . . . . .	22
		3.2.1.2 Rayleigh Approximation ( $d \ll \lambda$ ) . . . . .	23
	3.2.2	Stiffness and Force Calculations . . . . .	26
	3.3	Optical Trapping by Speckle Fields . . . . .	27
4		COFFEE-RING EFFECT . . . . .	31
	4.1	Drops on Substrates . . . . .	31
	4.2	Principles of Evaporating Droplets . . . . .	32
		4.2.1 Surface Tension . . . . .	32
		4.2.2 Contact Angle Phenomena and Wetting . . . . .	34
	4.3	Coffee-Ring Effect . . . . .	37
	4.4	Applications for Suppression of Coffee-Ring Effect . . . . .	38
5		EXPERIMENTAL RESULTS . . . . .	45
	5.1	Introduction . . . . .	45
	5.2	Materials and Methods . . . . .	46
		5.2.1 Experimental Setup . . . . .	46

5.2.2	Cleaning Procedure for the Glass Slides . . . . .	48
5.2.3	Sample Preparation . . . . .	48
5.2.3.1	Preparation of the Motility Buffer and Bacteria Culture . . . . .	49
5.2.4	Experimental Procedure . . . . .	50
5.3	Results without Optical Potential . . . . .	50
5.3.1	Droplets Containing Only Passive Colloidal Particles . . . . .	50
5.3.2	Droplet Containing Passive Colloidal Particles along with Active Particles . . . . .	51
5.4	Results with Optical Potential . . . . .	52
5.4.1	Droplets Containing Only Passive Colloidal Particles . . . . .	52
5.4.2	Droplet Containing Passive Colloidal Particles along with Active Particles . . . . .	53
5.5	Comparison of the Results and Discussion . . . . .	53
6	CONCLUSION . . . . .	61
	REFERENCES . . . . .	65

## LIST OF TABLES

### TABLES

Table 2.1	Classification of the Condensed Matter Systems . . . . .	10
Table 2.2	Basic calculation for figuring out the influence of particle size on the total surface area . . . . .	12

## LIST OF FIGURES

### FIGURES

Figure 1.1	Different kinds of stains. . . . .	2
Figure 1.2	Examples of evaporated and dried blood drops from four different individuals. . . . .	3
Figure 1.3	The effect of different shaped particles on the coffee-ring effect. . . . .	5
Figure 2.1	Solid vs. Liquid. . . . .	8
Figure 2.2	Biological and Artificial Active Brownian particles. . . . .	10
Figure 2.3	Fundamental properties of solutions suspensions and colloids acting as a bridge between these two mixtures . . . . .	11
Figure 2.4	The importance of surface area. . . . .	12
Figure 2.5	Tyndall Effect. . . . .	13
Figure 2.6	Brownian Movement. . . . .	15
Figure 2.7	Scheme showing various properties summarizing the separation of mixture types. . . . .	16
Figure 2.8	Optical microscope images of a mobile 10 $\mu\text{m}$ polystyrene particles and many <i>Serratia marcescens</i> bacteria attached to PS particles. . . . .	17
Figure 2.9	Trapping and transportation of a living motile bacterium. . . . .	18
Figure 3.1	The direction of reflected and transmitted beams. . . . .	19

Figure 3.2 A strongly focused laser beam is used in optical tweezers for the trapping of particles. . . . .	21
Figure 3.3 Display of the optical forces according to the ray-optics regime.	23
Figure 3.4 The forces originating in the Rayleigh regime for such a tightly focused laser beam. . . . .	26
Figure 3.5 Simultaneous dynamic multiple trapping of eight 2 $\mu\text{m}$ sized polystyrene beads in phase contrast created optical traps. . . . .	28
Figure 3.6 Multiple optical trapping example based on the speckle pattern for carbon particles. . . . .	29
Figure 3.7 Direct imaging through multimode fibers is prevented by mixing up the modes. . . . .	29
Figure 3.8 Transmitting a laser through a multimode fiber. . . . .	30
Figure 4.1 Photographs and Solidworks drawing of falling and landed water droplets. . . . .	31
Figure 4.2 Schematic representation of surface tension of a hemispherical water droplet on a solid flat surface. Purple arrows shows the intermolecular forces which molecules apply to each other . . . . .	33
Figure 4.3 Some examples for surface tension phenomenon. . . . .	33
Figure 4.4 Demonstration of the balance of interfacial tensions of a drop lying on a solid flat substrate. . . . .	35
Figure 4.5 Contact angle of a colloidal droplet on a substrate. . . . .	36
Figure 4.6 Image of water droplets on superhydrophilic and superhydrophobic surfaces. . . . .	36
Figure 4.7 Photograph of spilled coffee stains. . . . .	37

Figure 4.8 Demonstration of evaporation process of colloidal droplet falling on solid flat surface . . . . .	38
Figure 4.9 Dry deposits in different patterns as a result of evaporation of colloidal droplets. . . . .	39
Figure 4.10 Suppression of coffee-ring effect by hydrosoluble polymer additive. . . . .	40
Figure 4.11 Suppression of coffee-ring effect by shape-dependent capillary interactions. . . . .	41
Figure 4.12 Suppression of coffee-ring effect by acoustic waves. . . . .	42
Figure 5.1 Full view of the droplet after evaporation . . . . .	45
Figure 5.2 Schematic representation of the experimental setup. . . . .	47
Figure 5.3 Cleaning Procedure . . . . .	49
Figure 5.4 Experiment parameters tried before starting to take main results	51
Figure 5.5 Edge images of deionized water droplet consisting of 3 $\mu\text{m}$ polystyrene particles. . . . .	51
Figure 5.6 Edge images of deionized water droplet consisting of 3 $\mu\text{m}$ polystyrene particles and bacteria (motile <i>E. Coli</i> cells). . . . .	52
Figure 5.7 Edge images of deionized water droplet consisting of 3 $\mu\text{m}$ polystyrene particles. . . . .	53
Figure 5.8 Edge images of deionized water droplet consisting of 3 $\mu\text{m}$ polystyrene particles and bacteria (motile <i>E. Coli</i> cells). . . . .	54
Figure 5.9 Full images of deionized water droplet containing 3 $\mu\text{m}$ polystyrene particles. . . . .	54
Figure 5.10 Full images of deionized water droplet containing 3 $\mu\text{m}$ polystyrene particles and bacteria (motile <i>E. Coli</i> cells). . . . .	55

Figure 5.11 When no optical potential is applied (a) the passive particles tend to migrate towards the rim of the drop exhibiting the coffee-ring effect. The coffee-ring effect is suppressed when a random optical potential is applied over the drop (b). . . . .	55
Figure 5.12 When no optical potential is applied (a) the similar particles in active bath tend to accumulate at the air-liquid interface. The coffee-ring effect is completely suppressed when a random optical potential is applied over the drop area (b). . . . .	56
Figure 5.13 Comparison of results obtained with different techniques for the suppression of coffee-ring effect. . . . .	57
Figure 5.14 Effect of three different kind of solvents on coffee-ring effect.	58
Figure 5.15 Schematics of the simulation process. . . . .	59
Figure 5.16 A colloidal droplet evaporating on a flat substrate. . . . .	60



# CHAPTER 1

## INTRODUCTION

What we call "ordinary" and encounter in our everyday lives, in fact, has a very different place and significance in the world of science. Indeed, we are all aware of many things around us; however, we are so used to them that most of the time we are incapable of questioning them. For example; have you ever noticed the coffee-stain that has formed after a while as a result of a spilled coffee droplet? If you have noticed it, do you have any idea why and how it happened? This phenomenon, which we see as being very simple, has become the center of attention for many researchers in the physics world especially in recent years and contrary to expectations it is actually based on a surprising amount of basic physics and mathematics.

Starting from this point let's ask the following question: What happens if we evaporate a droplet including dissolved particles? I think it does not sound difficult. People who consume a lot of coffee, i.e. coffee drinkers, will be able to answer this question easily. After a spilled coffee drop dries on a substrate, a dark ring appears on the outside while leaving a lighter area of stain inside. The formation of these ring-like depositions at the outer boundary of the droplet is known as "Coffee-Ring Effect".

Because of its name it can be thought that this effect is exclusive to only coffee. However; any complex liquid consisting of suspended colloidal particles such as tears, blood, red wine, pumpkin soup displays this behavior after the evaporation process on a substrate [3]. It is shown in Figure 1.1 with some visual examples.

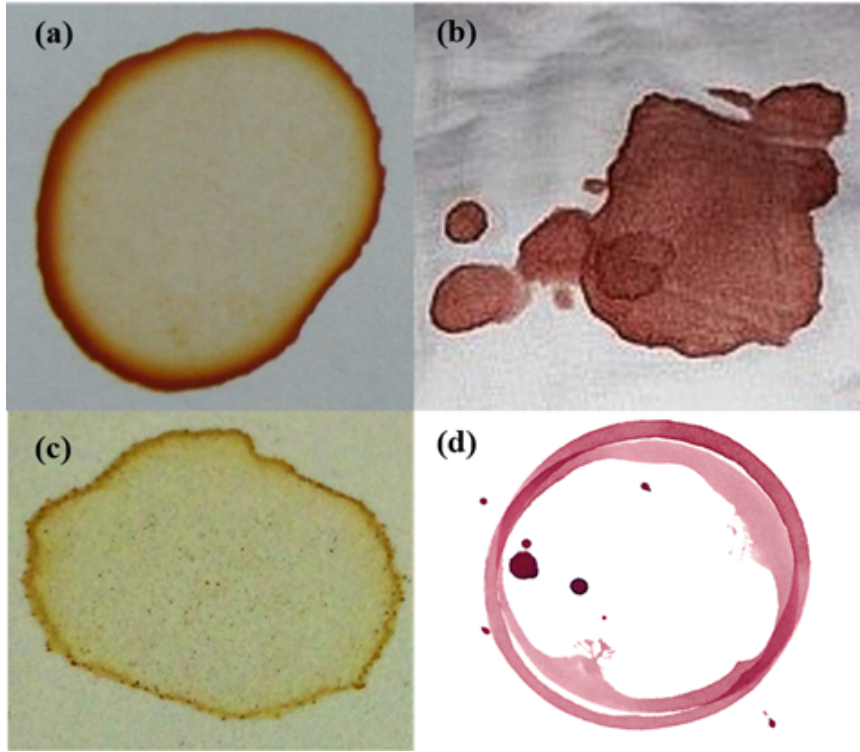


Figure 1.1: Different kinds of stains (a) coffee-stain [1] (b) blood-stain [2] (c) pumpkin soup stain [3] (d) red wine stain [4]

Now, let's take a look at the significance of this effect and its scientific uses. To be able to solve several problems in pure science and in emerging technologies such as multiple ring pattern formation [5], stretching and deposition of DNA [6, 7], DNA and RNA microarrays [7], optoelectronics [8], colloidal self-assembly [9], lithography [10], high resolution inkjet printing [11], thin films and functional coatings [7], medical diagnosis and drug discovery [12, 7], spotting methods for gene mapping and biochemical assays [7], chromatography [13] and many applications which requires the control of particle deposition, a full understanding of the coffee-ring effect has great importance [3]. With the help of this effect, various kinds of functional thin films for electronic circuits can be created by depositing metal particles. Also, localized areas with homogeneous and particular desirable characteristics can be created by using different kind of suspended materials in the droplets to arrange tiny crystals in the field of semiconductors developing techniques that enhance the efficiency of materials used in almost everything from electronics to solar energy harvesting [14]. Furthermore, in the detection of some certain diseases it is a very practical way to

observe dried body fluid deposits [15]. If you look at Figure 1.2, you will see four different image of evaporated blood droplets taken from healthy people, anaemic and hyperlipidaemic patients. As blood droplets evaporate and dry, difference in their cracks and shape can be observed. By this informant pathway obtained from the final deposits it can be determined whether the individuals who have donated blood samples are healthy or not. In Figure 1.2, (a) and (c) belong to healthy individuals, (b) depicts a person with anaemia and (d) indicates a person with hyperlipidaemia [16]. Many other similar examples can be given under the heading of applications where the coffee-ring effect is effective.

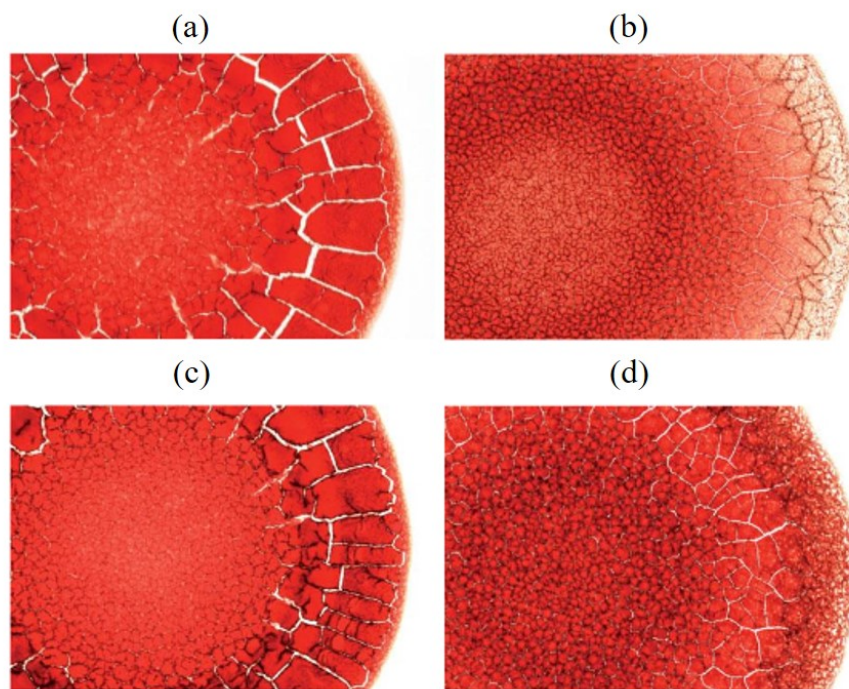


Figure 1.2: Examples of evaporated and dried blood drops from four different individuals (a,c) healthy individuals (b) individual with anaemia (d) individual with hyperlipidaemia [16]

As explained above, there are many applications and emerging technologies that benefit from the coffee-ring effect. On the other hand; there are also many industrial applications in which it is desirable to control and even overcome. It is not always a desirable and favored formation. For the sake of an example from biotechnology, examination of biological moieties such as DNA molecules or bacteria requires a homogeneous disc-like or concentrated deposition on a

substrate [3]. Therefore, many researches have been carried out research to attempt to suppress this coffee-ring effect for the control of the deposit pattern and there are various methods applied in this direction. In both cases where this effect is desired and undesired, how the stains are formed should be definitely known.

The formation of the coffee-ring effect is determined by three ingredients which are contact line pinning, nonvolatile solute and outward flow. Changing the flow caused by the fluid evaporating from the edge of the droplet is a general approach in the suppression of the ring stain to have a uniform and concentrated deposit. An irregular temperature profile is formed during the evaporation process and consequently, a surface tension activates the thermal Marangoni flow. Depending on this Marangoni effect, the movement of the surface liquid, the thickness and density of the resulting boundary line of the evaporated droplet alter. Therefore, the weaker the Marangoni effect, the denser the ring stain is formed. When it is strong, the particles at the stagnation point in which the direction of surface flow changes start to accumulate around the center of the droplet instead of the edges of it. [17] So, thanks to the applicable and developable methods in this direction it is possible to control and even overcome the coffee-ring effect.

Drying a droplet in a controlled and homogeneous distribution is not an easy process but it is not impossible. As the simplest method, with the provision of sufficient rapid evaporation conditions it may be possible to homogeneously deposit the particles in the interior rather than at the edge of droplet without making any changes to the droplet composition or the particles modification [18]. Another common method is changing the particle shape, which is illustrated in Figure 1.3. It has been observed while round particles accumulate at the drop edge by showing a common coffee-ring effect, elongated ones leave behind a disk-like concentrated uniform stain rather than a ring-like nonhomogeneous stain. Therefore, the behavior of the coffee stains can be changed by manipulating the particle shapes [19]. Another known method for suppression of the coffee ring effect is to benefit from hydrosoluble polymer additives [13] or surface acoustic waves (SAWs) [20]. These methods are explained in detail under the heading of ‘Applications’ in the coffee-ring effect chapter.

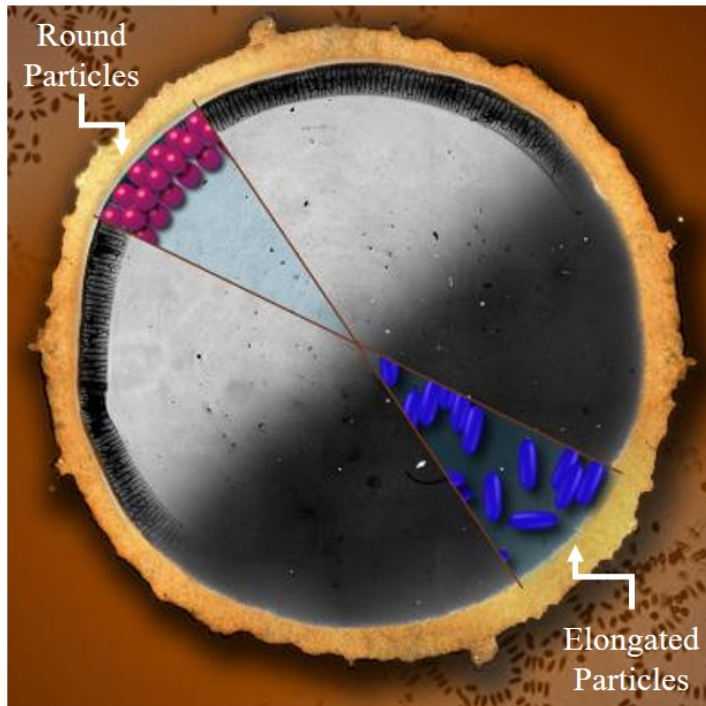


Figure 1.3: The effect of different shaped particles on the coffee-ring effect. Adopted from [21]

In the light of all this information, this thesis focuses on another method that we found to control and suppress the coffee-ring effect. I have investigated the effect of random optical potential application on a liquid droplets containing active and passive particles.



## CHAPTER 2

### CONDENSED MATTER PHYSICS

At the beginning of the 20th century, some fields concentrating on studying several aspects of solid matter such as magnetism, elasticity, metallurgy and crystallography gained importance among the other research fields of physics [22]. In the 1940s these fields started to be investigated under the new discipline of “solid state physics”. Then, just two decades later, investigation of the physical properties of liquids was also added to that area and a new comprehensive name, which is “condensed matter physics”, was given to that field [22].

Condensed Matter Physics (CMP) is one of the subfields of physics and physical properties of condensed phases of matter are investigated under that field. There are many practical applications taking advantage of this area. It is possible to give many research examples in a wide range of areas. The topics that condensed matter physics generally concentrates on includes magnetism, superconductivity, complex fluids, semi-conductors, thin films, photonic crystals, structure of ordered and disordered solids, nano-electronics and nano-optics [23]. Because of this extensive research field, CMP is by far one of the most important and the largest working areas of modern physics.

In order to be able to study condensed matter physics, we definitely need to understand different phases of matter, the relationship between the atoms such as forces and intermolecular attractions etc. Broadly speaking, states of matter available in nature can be classified into three different phases as solids, liquids and gases, which all are constituted by microscopic particles.

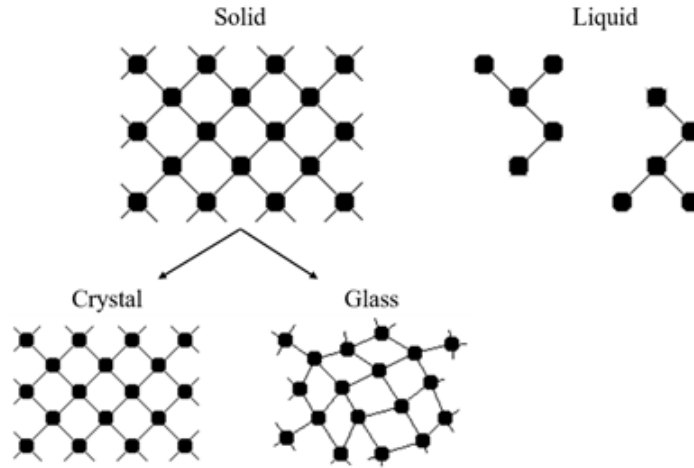


Figure 2.1: Solid vs. Liquid. Adapted from [24]

As can be seen from the Figure 2.1, while solids have a rigid structure and their bonds are stable, liquids have a flexible structure and, bonds breaking and forming dynamically. Solids can also be divided into two categories as crystal, which has a regular repeating pattern, and glass, whose particles are not arranged in a regular pattern [24]. Because of the strong particle interactions and intermolecular forces due to the closeness of the particles to each other, solids and liquids are often referred to as “condensed matter”. Depending on the type of the material of interest, condensed matter is generally examined under the different headings by subdividing into two categories which are “hard” and “soft” condensed matter [24].

## 2.1 Hard Condensed Matter

Hard and soft condensed matter, which make up the condensed matter physics, can be distinguished from each other by the role of quantum mechanics for the elementary excitations of the systems. In soft condensed matter physics, which studies the statistical mechanics of biomolecules, liquid crystals, gels, polymers, colloids etc., classical mechanics is sufficient to comprehend the motion and accumulation of the systems[25]. On the other hand, classical dynamics is not sufficient in studying hard condensed matter physics and therefore, quantum mechanical rules go into effect. Because of that, the term “ $\hbar=0$ ” physics is used for defining soft condensed matter physics and the term “ $\hbar=1$ ” physics

is utilized for hard condensed matter physics in which lattice vibrations and electrons' motion are determined by Schrödinger's equation [25].

## **2.2 Soft Condensed Matter**

The term “soft matter” or “soft condensed matter” is used to describe a large class of materials, which are easily deformed with the effect of external forces and thermal fluctuations, in the state of matter that is neither basic liquid nor crystalline solid [26, 27]. Instead of “soft matter” term, there are some other synonym terms that can be used as “colloidal suspensions”, “colloidal dispersions” or “complex fluids” even though the soft matter does not have to be fluid [26, 27]. Surfactants, polymers, gels, colloidal suspensions, active matter such as bacterial suspensions and biological polymers can be shown in the scope of that subfield of physics [28, 29, 30, 31]. From the combination of the words “glue” and “kind” Greek-origin term “colloid”, which means “sticky stuff”, came out in the 1861 by Thomas Graham. [32]. Soft matters can be investigated in two categories in itself as active and passive soft matter.

### **2.2.0.1 Active and Passive Soft Matter**

There are a lot of colloidal particles that make up the soft matter and they can be characterized by their electrical, optical, structural, mechanical and chemical properties. It is possible to collect all of them under two fundamental frameworks namely “passive” particles moving with the effect of external forces and torques, and “active” particles self-propelling by gaining kinetic energy from their surroundings and by converting it into directed motion, also known as self-propelled micro swimmers [26, 33, 34]

Active colloids can be further grouped into two categories which are natural ones in the form of micro-organisms, can be called as biological micro swimmers, and synthetic self-propelled particles, can be termed artificial swimmers [33]. These biological or man-made microscopic or nanoscopic active Brownian particles have great importance in the studies of physical and biophysical field [36].

Table 2.1 summarizes the classifications mentioned so far.

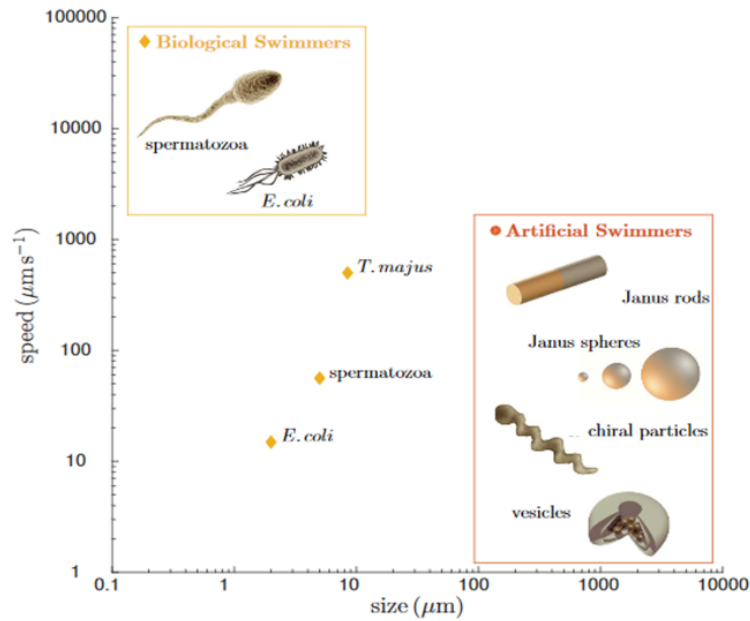


Figure 2.2: Biological and Artificial Active Brownian particles. Their sizes are in the range of micro and nano scale. They have propulsion speeds up to a fraction of a millimetre per second. Adapted from [35]

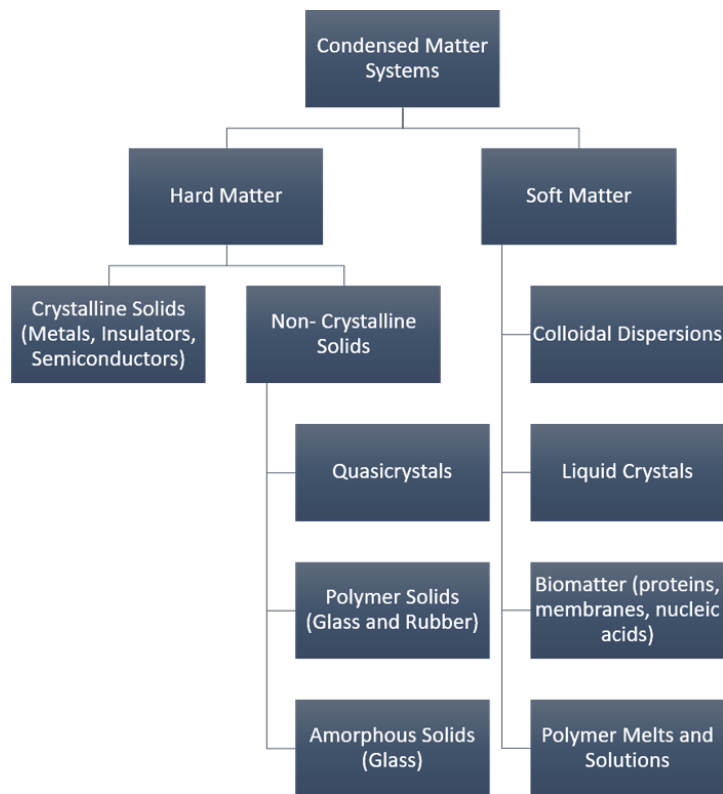


Table 2.1: Classification of the Condensed Matter Systems

### 2.3 What makes colloidal particles so special?

Colloids acting as a bridge between the microscopic and macroscopic scale are in the middle between particulate suspensions and solutions with respect to particle size and their optical properties [37]. They are composed of two phases: the dispersed phase consisting of small insoluble colloidal particles and the dispersion medium including colloidally dispersed and suspended particles.

Colloids, which can be made from solid, liquid and gas, looks as homogeneous but in reality they are heterogeneous mixtures consisting of particles in size between 1-1000nm. Since the dispersed particles are very small, when viewed from afar it seems as homogeneous. However; when it is observed closely under the light, particles inside can be seen easily. Blood, starch-water mixture, smoke, fog, foam, milk, mayonnaise, muddy water, paint, dust cloud can be given as an example to that [38].

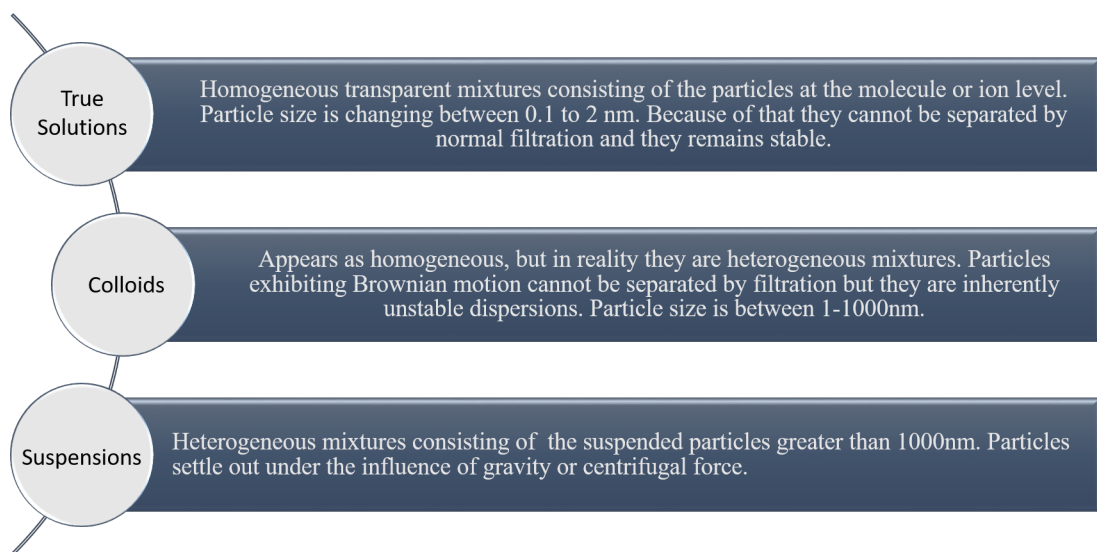


Figure 2.3: Fundamental properties of solutions suspensions and colloids acting as a bridge between these two mixtures

What makes colloidal particles so special is three characteristic features which are particle shape and flexibility, surface chemical and electrical properties, and most importantly the particle size. Particle surface area defines the effectiveness of a colloid and the particle size also plays a role in determining the surface area of the particle [39]. As particles are getting smaller, surface area starts to be

greater. When a solid is sliced up to smaller pieces, more surface is obtained with the same preserved total mass but altered total surface area. Because a large number of smaller new surfaces are created, surface area to mass ratio become tremendously large. Therefore, the smaller the particle sizes, the larger the surface area.

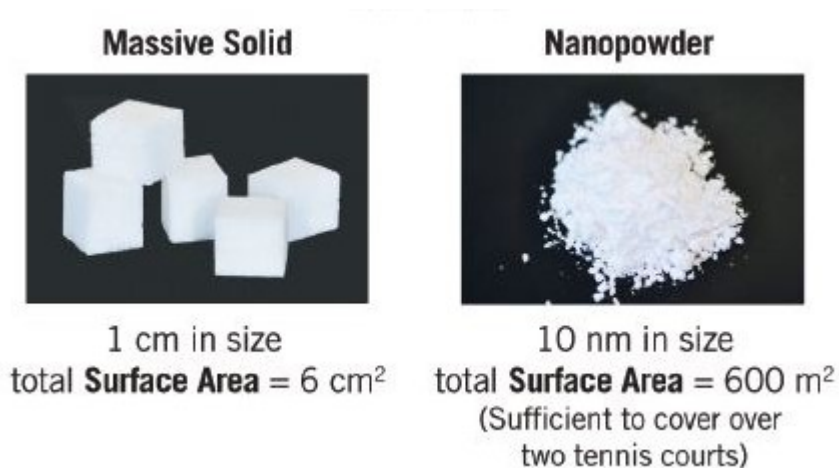


Figure 2.4: The importance of surface area [39]

# of slices per cube face	Length of each face (cm)	Surface area per face	# of cubes	Total surface area
$n$	$1/n$	$n^{-2}$	$n^3$	$6n \text{ cm}^2$
100	0.01	$10^{-4} \text{ cm}^2$	$10^6$	$600 \text{ cm}^2$

Table2.2: Basic calculation for figuring out the influence of particle size on the total surface area

Why we are so interested in surface area is that surfaces or interfaces between phases have their own physical and chemical characteristics, which are generally hidden from us because of the limited amount of surface area in relation to the quantity of matter in bulk matters. So the result that we are supposed to extract from here is that while the colloidal solids sizes are getting smaller, the features of their surfaces starts to dominate their behavior [37].

### 2.3.1 Properties of Colloidal Dispersions

Colloidal systems display remarkable optical, mechanical and electrical characteristics.

### 2.3.1.1 Optical Property: Tyndall Effect

Distinctive aspect of colloidal dispersions from true solutions is their light-scattering features. While a beam of light passing through a colloid is scattered by the particles in the light path which is visible, light passing through a true solution such as salt in water, ethanol in water, air, sucrose dissolved in water is scattered so little in the path which cannot be observed and the amount of light scattered cannot be detected without the help of sensitive instruments. This phenomenon is known as Tyndall effect, which is the result of light scattering by colloids, and it is discovered by John Tyndall in 1869 [40]. This effect can be observed solely in colloids, not in true solutions.

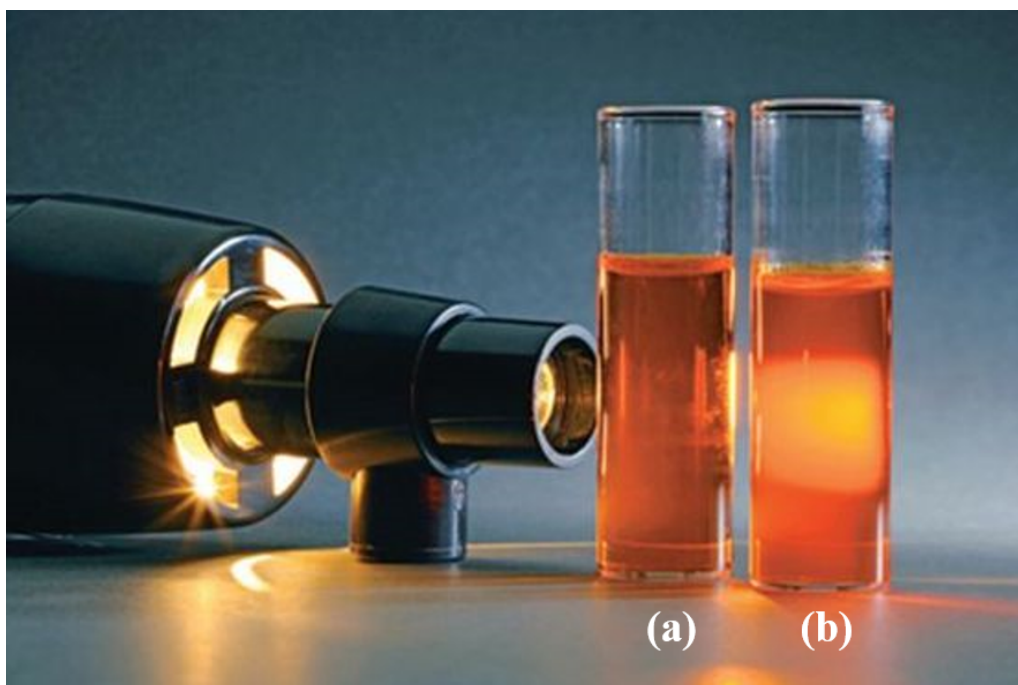


Figure 2.5: Tyndall Effect (a) True solution: beam of light is transmitted with some reflection on the test tube glass. There is no scattering inside. Path of light cannot be seen (b) Colloid: beam of light scatters off surfaces of suspended particles. Path of light becomes visible [42]

Tyndall effect and Rayleigh scattering are very comparable to each other. The size of the particles defines the intensity of Rayleigh scattering. It is proportional to the fourth power of the frequency, which means that the longer wavelengths of the visible spectrum is scattered weaker than the shorter wavelengths. According to that effect, the shorter wavelength light is more reflected through scattering

while the longer wavelength light is more transmitted [41]. It is something that can be seen in our daily life. For instance, what gives rise to the sky to seem to be blue is the Tyndall effect. After sunlight penetrates the Earth's atmosphere and travels through millions of small particles in the air like dust and various debris, it is scattered; and because the shortest wavelength belongs to blue color, the sky is seen as blue preponderantly [43]. Also, while shortwave electromagnetic waves such as light waves are obstructed and reflected by the walls, longwave electromagnetic waves such as radio waves are able to penetrate into the walls of buildings [41].

### **2.3.1.2 Kinetic Property: Brownian Motion**

Since the early of 19th century various scientific studies on colloids have been carried out and the one that can be shown among the first striking works was done by British botanist Robert Brown [44]. Because of their sizes, it is not possible to observe them under an ordinary optical microscope. That's why for the observation of colloidal particles a special microscope was designed, which is known as an ultramicroscope invented in Austria in 1902 [45]. Thanks to that microscope, particles still cannot be seen directly but the location of the particles can be defined with the scattered light at any given instant. When colloidal particles are observed under an ultramicroscope, it is seen that the particles are making a continuous and rapid zig-zag motion, which is named as Brownian movement [37].

As can be seen in Figure 2.6, as a result of the collision of particles, they are directed to different directions by the effect of driving force. When the particle moving in one direction collides with another one, its direction changes and this process goes on like this. Random zig-zag movements of the colloidal particles are formed in that way. Particle size and the viscosity of the dispersion medium are two important parameters defining the intensity of that random motion. The lighter the particles and the less viscous the dispersion medium, the faster the motion. Correlatively, the heavier the particles and the more viscous the dispersion medium, the slower the Brownian motion. This constant motion causes the stabilization of colloidal solution to a certain extent by preventing

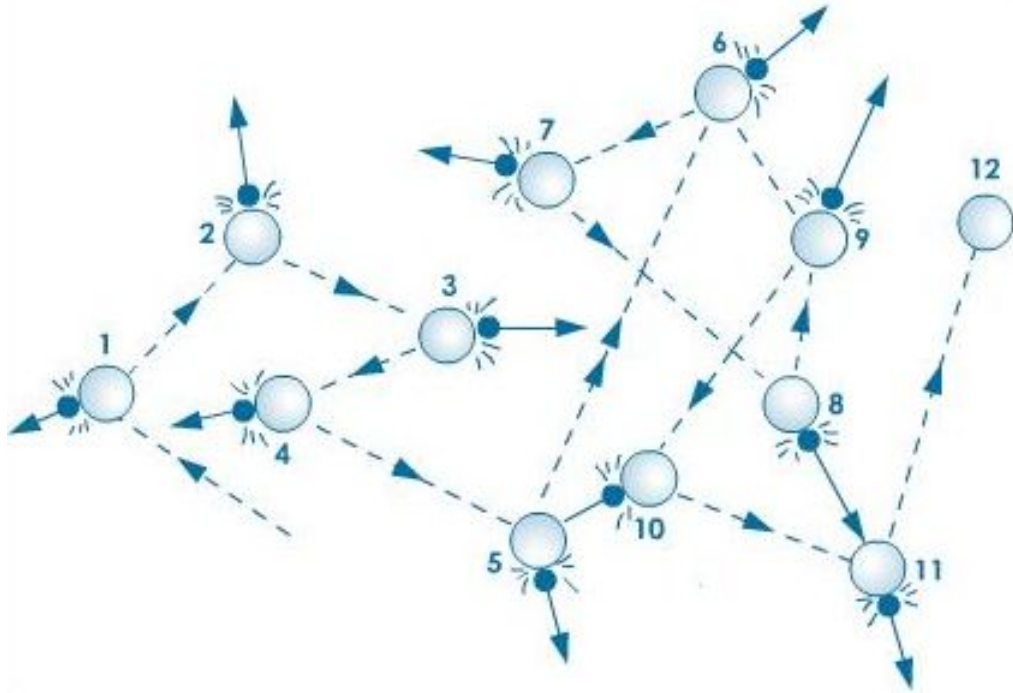


Figure 2.6: Brownian Movement [46]

the particles from settling down because of the gravitational forces affecting the colloidal particles [40].

### 2.3.1.3 Electrical Properties

Another important property of colloidal particles constituting the dispersed phase is that they are electrically charged with respect to the dispersion medium, therefore there is always difference in electric potential between the colloid phase boundaries. Because all of these colloidal particles carry electric charge with the identical sign, there happens a repulsive electrostatic force between them as we understand from the Coulomb's law which is one of the fundamental rules of physics. That's why the particles can remain dispersed in the dispersion medium. So, when they are put under an electric field, colloidal particles are forced to migrate towards the oppositely charged side [47]. This phenomenon is called as electrophoresis and with that method separation of a colloidal mixtures such as protein can be possible [48].

So, what has been written so far can be summarized with a scheme as shown in Figure 2.7. Some information, which helps us in determining the mixture type

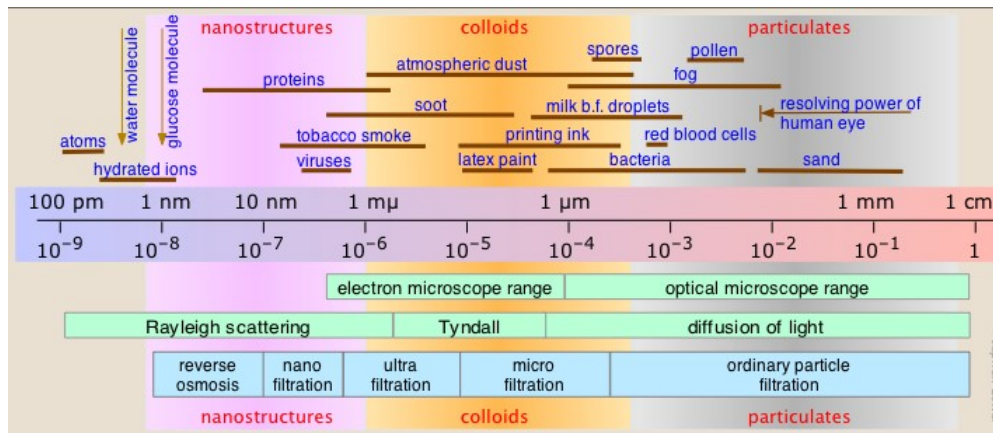


Figure 2.7: Scheme showing various properties summarizing the separation of mixture types [37]

and separates the particulate suspensions, solutions and colloids, such as particle size scale, filtration type and optical properties that make them recognizable is collected under a common scheme.

### 2.3.2 Applications

Active and passive soft matters play a very crucial role in nature and our daily life, e.g. medicines, purification of water, photography, smoke precipitation, rubber industry and etc. For example, by utilizing the electrical properties of colloidal particles, it is possible to dispose the sewage water. When that water is put under the high potential, thanks to the electrophoresis characteristic of colloidal particles, they are coagulated and only pure water remains by removing the suspended matter [49].

Passive and active Brownian particles contribute to science with their characteristic properties. Many researches are carried out by taking advantage of these particles and let's give them some examples (see Figure 2.8 and Figure 2.9).

It has been demonstrated that bacterial flagella can perform the same function as nano actuators for swimming at micro scale by Bahareh Behkam and Metin Sitti from Carnegie Mellon University. Microscale objects are propelled forward with the effect of collective propulsion force created by bacteria's flagellar motors as a result of adhesion of the bacteria to that objects. By controlling the rotation

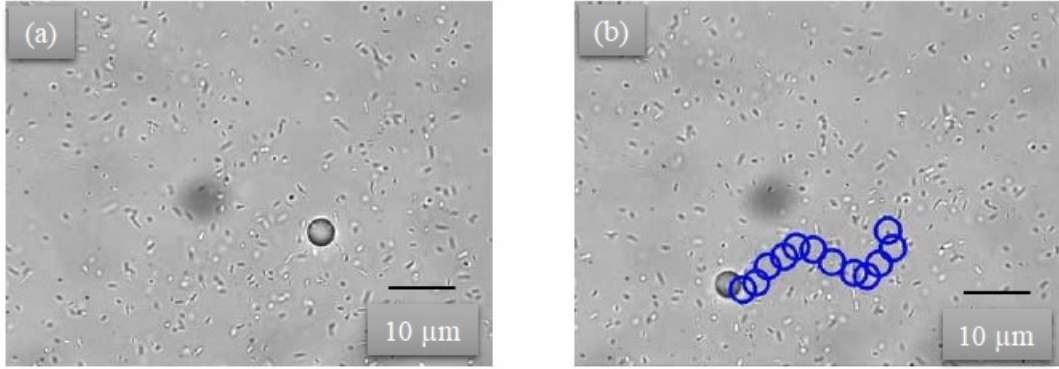


Figure 2.8: Optical microscope images of a mobile  $10\ \mu\text{m}$  polystyrene particles and many *Serratia marcescens* bacteria attached to PS particles (a)  $t=0$  and (b)  $t=6\text{s}$  [50]

of that flagellar motors of bacteria it has been shown that it is possible to manipulate the motion of such microscale objects [51]. While in that research there was a random adhesion of bacteria over the whole surface of microbeads, in another research shown in Figure 2.8 to be able to regulate where bacteria attaches to the bead and to make better the effectiveness of the propulsion and the motion directivity, the microbeads are patterned.

With that method, they observed that patterned beads have more efficiency than unpatterned ones and moving with approximately the similar speed for half of the number of attached bacteria. The other advantage is this method enabled to have improved directivity of motion by nearly 25%. Also, they investigated the effect of bead size on the attachment density and thus the propulsion force [50]. So, they concluded that this work may lead other studies for micro-robotic applications by understanding the hydrodynamics of bacterial flagellar propulsion.

And in their next study, a stochastic dynamic model of previous work has done by Veaceslav Arabagi and Eugene Cheung in addition to first two authors. Miniature mobile robots have a great importance in minimally invasive diagnosis and their treatments in the human body, environmental monitoring, search and rescue, security and in many other applications in terms of enabling us to reach small areas and working in parallel with numerous agents through distributed control. In the works initiated by way of these thoughts, it has been

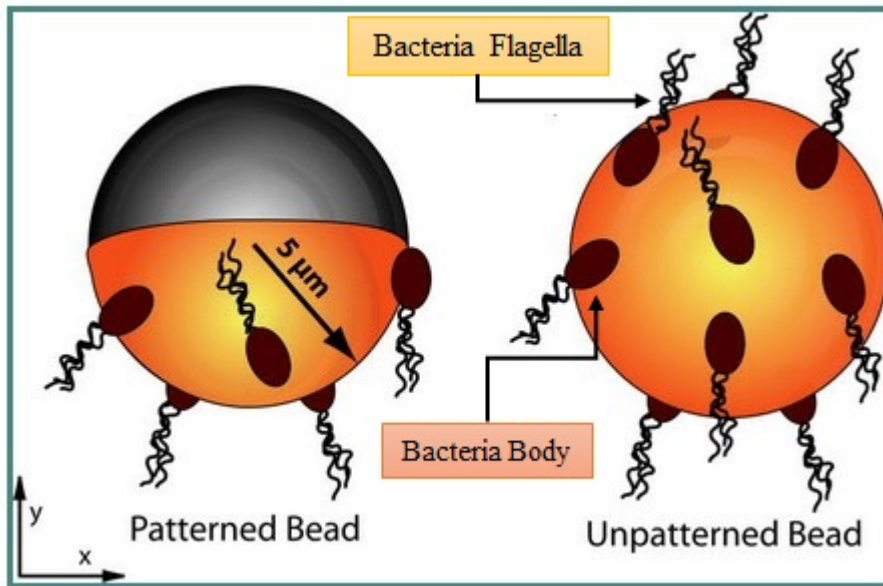


Figure 2.9: Trapping and transportation of a living motile bacterium [52]

seen that flagellated bacteria is used as actuators in liquid medium and so self-propelling bacteria can be used as swimming microrobotic bodies by attaching spherical microbeads. With the stochastic model improved for that study it is supposed to enable us a possibility for future potential targeted drug delivery and disease diagnosis applications of bacteria propelled microrobots [52].

## CHAPTER 3

### OPTICAL TRAPPING

#### 3.1 Introduction



Figure 3.1: The direction of reflected and transmitted beams. Adapted from [54]

When a laser beam is directed through a huge transparent object, such as prism displayed in Figure 3.1, there occurs a back reflection of a fraction of the power of a laser beam and the rest penetrates through the prism and exits from the other side. According to the Newton's action-reaction law, because of the difference in the direction of laser beams incoming, reflected and transmitted, there happens a change in the mechanical momentum, which results in a force on the object. It was already proved by Arthur Ashkin, who has been seen as the father of optical trapping field, that microscopic particles can be speeded up with the effect of the force of radiation pressure from a continuous laser and can be confined in 3D dimension as well, which forms the basis of optical tweezers [53]. How to

identify the laser beam is possible by thinking it as an accumulation of light rays for using geometrical optics which has taken advantage of calculating the optical forces. It provides an ease while studying with the object of interest that are comparatively greater than the wavelength of light, like cells and huge colloidal particles whose size is generally importantly larger than one micrometer [54].

The ability to remotely control matter with lasers is playing a great role in biology and physics. Optical tweezers produced by utilizing radiation pressure from a single laser beam were first realized in 1986 by Arthur Ashkin and co-workers at the Bell Telephone Laboratories [55, 56]. They published a paper which is titled as “Observation of a single-beam gradient force optical trap for dielectric particles”. This technique is now termed as “optical tweezers” or “optical trapping” [55]. In principle, for manipulating and applying forces to submicron particles, *E. coli* flagella [57], single kinesin motor [58, 59] and cytoplasmic dynein [60], optical traps use light and for that purpose the radiation pressure from a focused laser beam is used. In addition, information about the position of the object in the laser focus is obtained by measurements of the light deflection. Optical tweezers are very useful tools for studying biological systems in terms of the picoNewton and nanometer ranges of force and distance accessible to optical traps [56].

### 3.2 The Physics behind the Optical Trapping

The interaction of light with matter constitutes the most basic idea behind optical trapping. When Ashkin did the optical trapping experiments in 1986, he noticed that objects with high refractive index moves towards the center of the beam with an unfocused laser beam in the direction of propagation, and then he realized that in three dimension thanks to a single tightly focused laser beam small spherical dielectric particles could be captured [55].

When light interacts with the object, some fraction of its momentum is transferred to the object and there happens an axial force on it by momentum conservation. As shown in Figure 3.2, the particle captured in optical trap displays a Gaussian distribution created by harmonic potential characteristic of electric

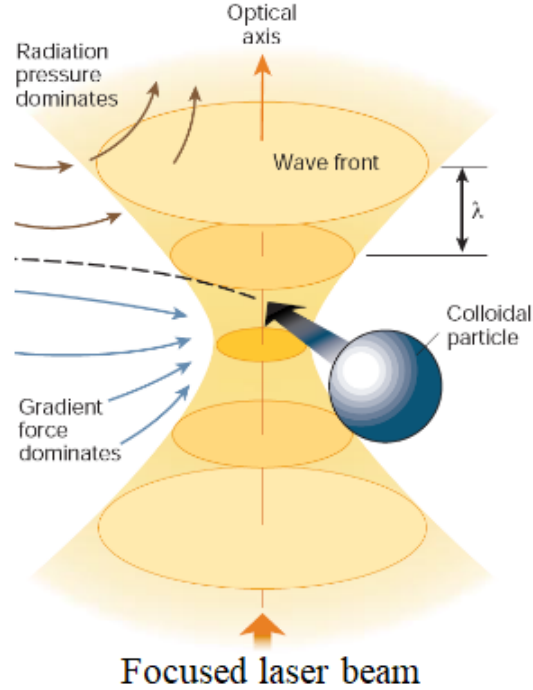


Figure 3.2: A strongly focused laser beam is used in optical tweezers for the trapping of particles [61]

field due to the focused laser. What is needed for a stable and homogenous trapping force on a particle is first the laser producing a collimated, monochromatic, coherent Gaussian beam so that light can be focused to a diffraction limited spot by the microscope objective [62], and secondly a high numerical aperture objective providing a steeper light rays and so a stronger axial trap [63].

### 3.2.1 The forces generated by optical tweezers

Every photon carries momentum  $h/\lambda$  and energy  $h\nu$ , so when the object absorbs the light, the momentum transferred from a light beam of power  $P$  gives rise to a reaction force  $F$  on the object, calculated by

$$F = \frac{nP}{c} \quad (3.1)$$

where  $n$  is the refractive index of the medium and  $c$  is the light velocity. The forces generated by optical tweezers can be described with two distinct approaches which are ray optics model in case particles at least 20 times larger

than the wavelength of light ( $d \gg \lambda$ ) and the dipole approach in case particles smaller than the wavelength of light ( $d \ll \lambda$ ) [55].

### 3.2.1.1 Ray Optics Approximation ( $d \gg \lambda$ ) (Mie-Regime)

In that approach for finding the scattering and gradient forces particles trapped should be greater than the wavelength of light ( $d \gg \lambda$ ) and their refractive index should be smaller than the surrounding medium. By using ray optics, the component forces can be modeled [64]. Here, the shape of the particles matters and it is generally spherical. Intensity, momentum and direction rays described by geometric optics individually compose an incident monochromatic collimated laser beam [64].

Thus, by using ray optics it is possible to calculate straightly the optical forces which are scattering  $F_{scat}$  and gradient  $F_{grad}$  for a uniform dielectric spherical particle:

$$F(scat) = \left[ \frac{n_m \cdot P}{c} (1 + R \cos(2\theta_R)) \right] - \left[ \frac{T_F^2 (\cos(2\theta_R - 2\theta_T) + R \cos(2\theta_R))}{1 + R^2 + 2R \cos(2\theta_T)} \right] \quad (3.2)$$

$$F(grad) = \left[ \frac{n_m \cdot P}{c} (1 + R \sin(2\theta_R)) \right] - \left[ \frac{T_F^2 (\sin(2\theta_R - 2\theta_T) + R \cos(2\theta_R))}{1 + R^2 + 2R \cos(2\theta_T)} \right] \quad (3.3)$$

where  $R$  and  $T_F$  are the Fresnel coefficients, and  $\theta_R$  and  $\theta_T$  are the angles for reflection and transmission of the incident rays.

In Figure 3.3, the laser focus point and the particle is illustrated with red region and blue ball respectively. Also, light rays are represented with the black arrows and their intensities is shown with the thickness of these arrows. Thanks to them, forces acting on the particle and the direction of movement of the particle with the effect of these forces can be seen in detail. In the case that the laser is tightly focused, force can be generated to make the particle move towards the laser focus point, which results in a three dimensional trap with a single laser beam. In addition, the direction of the force resulting from refraction is related

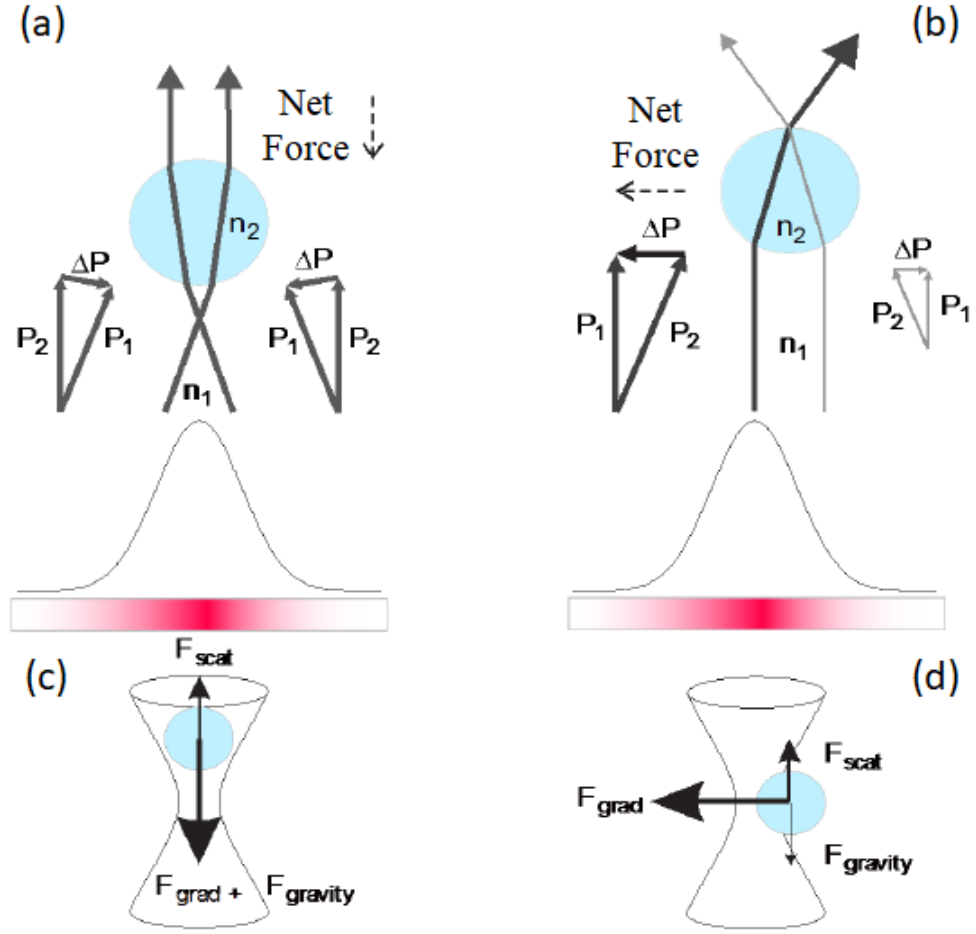


Figure 3.3: Display of the optical forces according to the ray-optics regime. The summation of the rays provides an (a) axial force owing to the vertical displacement from trap centre; (b) radial force owing to the lateral displacement from trap centre. Taking into account gravity and scattering, (c) the axial and (d) radial gradient force must be the dominant component to form an optical trap [64]

with the intensity of the laser beam instead of the direction of propagation. So, it can be concluded that the reversing of the light ray direction does not cause any change in force direction [55].

### 3.2.1.2 Rayleigh Approximation ( $d \ll \lambda$ )

It is the case where the particle size trapped is smaller than the wavelength of laser beam ( $r \ll \lambda$ ) and here instead of the ray optical approach it is much suitable to think the forces resulting from refraction with regard to the electric field near the trapped particle. As in the first case which is Mie regime, here

also we can divide the forces into those caused by an intensity gradient and scattering of the light [55].

Because of the polarizability of the atoms or ions light coming upon a particle generates a dielectric response. So, the induced dipole moment is;

$$\vec{p} = \alpha \cdot \vec{E} \quad (3.4)$$

And then the electrostatic potential is generated from the result of an interaction between the induced dipole moment and light's electric field;

$$U = -\vec{p} \cdot \vec{E} \quad (3.5)$$

So the gradient force is;

$$\vec{F}_{grad} = -\vec{\nabla}U = -p \cdot \vec{\nabla}\vec{E} = -\alpha(E \cdot \nabla)\vec{E} \quad (3.6)$$

For a small particle of radius  $r_p$ , it leads to the force relation;

$$\vec{F}_{grad} = -\frac{n_m^3 \cdot r_p^3}{2} \left( \frac{n_c^2 - 1}{n_c^2 + 1} \right) \nabla E^2 \quad (3.7)$$

where  $n_m$  is medium refractive index,  $n_c$  is ratio of the refractive index of the particle  $n_p$  to the index  $n_m$  of the surrounding medium, and  $\alpha$  is written in open form valid for a small particle in an aqueous medium. According to the description of *Clausius-Mossotti* relation, spatial alteration of light field intensity and the dielectric contrast of the trapped particle considering the surrounding medium are two important terms to define the gradient force [55, 64]. So, from that equation the following conclusion can be reached that the force is directed towards the area which has the highest intensity of light.

Also there is another force caused by the scattering of light, which is a result of photons having momentum. It is called scattering force acting in the direction

of light propagation and depending on the light intensity instead of the gradient. The momentum of a single photon of energy  $E$ ;

$$\vec{p} = \hbar \cdot \vec{k} = \frac{\vec{E} \cdot n_m}{c} \quad (3.8)$$

Scattering from the particle causes two impulses in the light propagation direction and in the opposite direction of scattered photon. By thinking that the photon flux colliding with and quitting an object under the momentum conservation we can compute the change in momentum, or force in the following way;

$$\vec{F}_{scat} = \frac{\hat{n}}{c} \iint (S_{in} - S_{out}) \cdot d\vec{A} = \frac{\hat{n}_m \sigma \langle S \rangle}{c} \quad (3.9)$$

where  $S$  is the time-averaged Poynting vector,  $c$  is the speed of light,  $\sigma$  is the optical cross section of particle. For a small (than the light wavelength), spherical, dielectric particle, the Rayleigh scattering cross-section is shown as;

$$\sigma = \frac{8}{3} \pi \left( \frac{2\pi n_m}{\lambda} \right)^4 r_p^6 \left( \frac{n_c^2 - 1}{n_c^2 + 2} \right)^2 \quad (3.10)$$

where  $r_p$  is the particle radius. So, the scattering force on a Rayleigh particle can be written in terms of the light intensity  $I_0$ ;

$$F_{scat} = \left( \frac{128\pi^5 r_p^6}{3\lambda^4} \right) \left( \frac{n_c^2 - 1}{n_c^2 + 2} \right) \frac{n_m}{c} I_0 \quad (3.11)$$

As can be seen from the Figure 4, in the case of a highly focused laser beam, there is a component forming the gradient force, which is the one against the Poynting vector, for preventing the particle from being pushed in the direction of light propagation by the scattering force. Also, the net force performs as a restoring force toward the laser focus point [65].

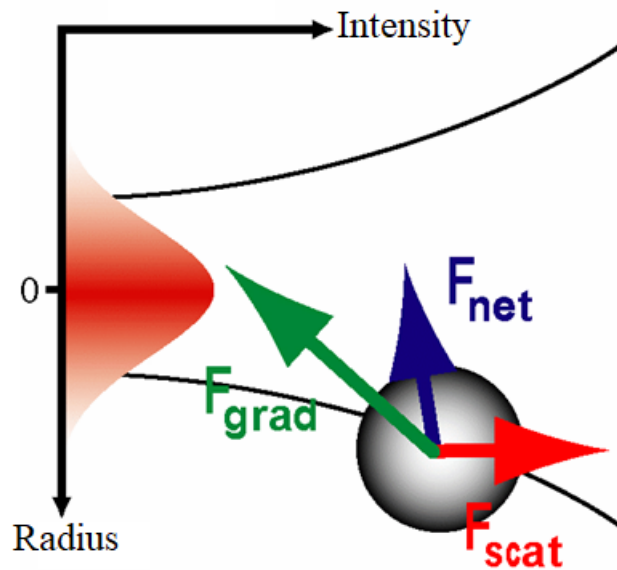


Figure 3.4: The forces originating in the Rayleigh regime for such a tightly focused laser beam [65]

### 3.2.2 Stiffness and Force Calculations

A bead captured with optical tweezers behaves like an object attached to a spring. In practice, the bead is continuously moving with Brownian motion, which is the random motion of particles suspended in a fluid caused by their collision with the quick atoms or molecules in the medium as mentioned in previous chapter in the “Kinetic Property: Brownian Motion” part. But whenever it leaves the optical trap center the restoring force pulls it back to the center. When an external force is applied to the trapped bead, the optical trap acts like a spring by recoiling back and pulling the bead back to the focus. The force which the trap pulls the bead back can be determined using Hooke’s law:

$$F = -k.x \tag{3.12}$$

where  $k$  is the stiffness of the trap and  $x$  is the bead displacement resulting from the applied force.

### 3.3 Optical Trapping by Speckle Fields

Optical tweezers play a great role in a wide range extending from many physical and biological studies to medical science and nanoscience in terms of their manipulation and control capability for assembly of micro and nano sized dielectric particles, cells, sub-cellular structures and DNA-molecules [66]. Besides single-beam optical tweezers, sometimes a multiple optical trapping system is required when an array of particles has to be captured at the same time and manipulated separately. For that purpose, multiple tweezers can be generated by increasing the number of laser light sources [67], which is a very basic but overpriced way, by splitting the single laser into a number of trapping positions [68], which can be achieved with the use of beam splitters or gratings for a restricted number of traps, by using scanning mirrors [69] and acousto-optic modulators [70] for advanced experiments, and by creating multiple beams through dynamic diffractive optics [71], which is typically in the form of a computer controlled spatial light modulator (SLM) used for creating holograms to modify the phase or beam intensity.

As can be seen from the Figure 3.5, eight polystyrene micro particles (two inside and six outside) are trapped simultaneously in defined phase pattern that is addressed on the spatial light modulator and also dynamically manipulated in the limit of response time of liquid crystals in SLM. In several experiments done at Risø National Laboratory in Denmark Technical University, they have demonstrated a technique for multiple trapping of micron-sized particles by using the generalized phase contrast approach with a phase-only SLM. Thanks to that approach done with the help of a simple PC-interface, managing of the number, location, shape, size and speed of the traps is possible [72].

Another strategy to obtain a multiple optical trapping with a single laser beam is to create speckle patterns and so speckle fields. Such systems are called “speckle optical tweezer” and the simplest way to generate these speckles, which are random light fields, is the coherent laser light scattering happening in optically complex media like biological tissues, rough surfaces and disordered structures. In that way naturally random diffraction patterns are produced to manipulate

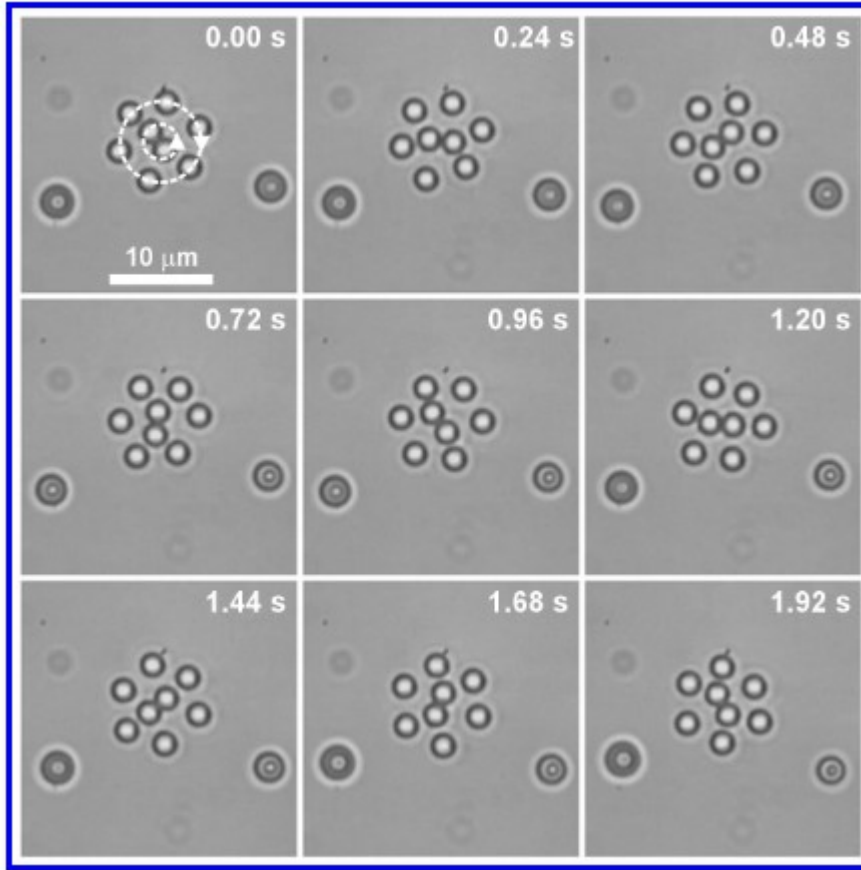


Figure 3.5: Simultaneous dynamic multiple trapping of eight  $2 \mu\text{m}$  sized polystyrene beads in phase contrast created optical traps. Laser power incident on the SLM is 60 mW and for each trap is 1.3 mW. They are rotating in opposite directions with different speeds. While the two micro particles inside the circle are doing one full rotation counter clockwise, other six micro particles outside the circle making  $1/8$  of a full rotation in opposite direction. Also, two particles apart from these 8 particles you see are making Brownian motion freely because they are not under the influence of radiation pressure. [72]

many particles simultaneously [73]. Also by using different types of diffuser and holograms thanks to SLM it is possible to obtain desired speckle patterns as shown in Figure 3.5 and 3.6. With that experiments it has shown that multiple trapping, holding and sorting for light absorbing numerous particles are possible by creating different speckle patterns. By increasing the number of optical trap locations and the particles trapped many different optical trapping experiments can be carried out in parallel, and also larger arrays of cells or colloids can be studied.

Lastly, another way to generate speckles is to use multimode fiber, which is

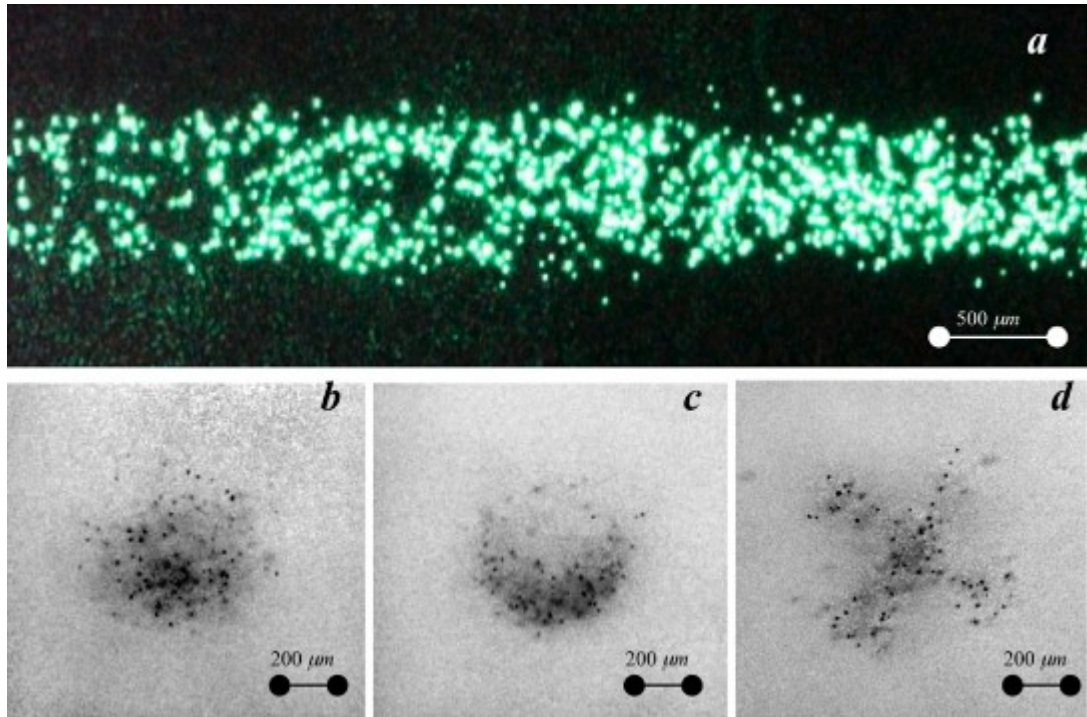


Figure 3.6: Multiple optical trapping example based on the speckle pattern for carbon particles. (a) side view of the laser light scattering from a great number of trapped carbon particles ((b)-(d)) axial views for different illuminated beam shapes on the diffuser (b) a Gaussian beam (c) a doughnut-like beam (d) a cross-like beam shape. For these experiments shown respectively from a to d the total laser power used is 115 mW [74]

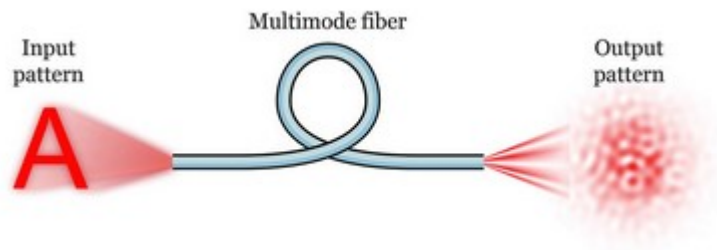


Figure 3.7: Direct imaging through multimode fibers is prevented by mixing up the modes [75]

also a technique carried out in this thesis study. Compared with single-mode fibers, multimode fibers offer several paths (modes) inside to travel for light. That's why this term "multimode" is coming from here. When coherent laser light enters from one side of the multimode fiber, the output displays a pattern of light and dark spots called as speckle pattern caused by constructive and destructive interference of light. That's why the image sending through the fiber

leaves as blurred as shown in Figure 3.7 because it takes several hundred ray paths possible inside the core of the fiber during its travel [75]. Because of these different eigenmodes of the fiber, optical waves interfere with random phases and thus there happens random speckle patterns, which can also be changed by bending of the fiber, at the end of the fiber tens or hundreds of meters away from the laser like in Figure 3.8 [73, 76].

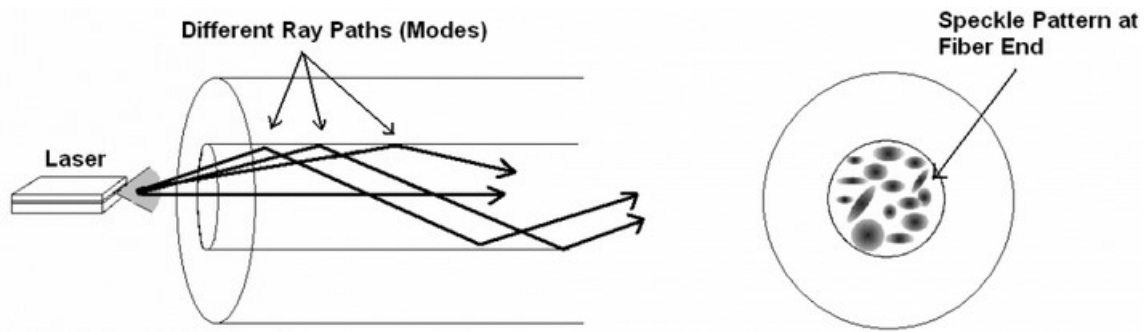


Figure 3.8: Transmitting a laser through a multimode fiber [76]

## CHAPTER 4

### COFFEE-RING EFFECT

#### 4.1 Drops on Substrates

When a drop of water is positioned on a solid flat surface, the drop may spread out entirely or partially or may rest on the substrate like a solid sphere depending on the interactions between the liquid and the surface, and some properties of them. Density, viscosity, elasticity and surface tension are some fundamental characteristics defining the liquid type and also the flow pattern.

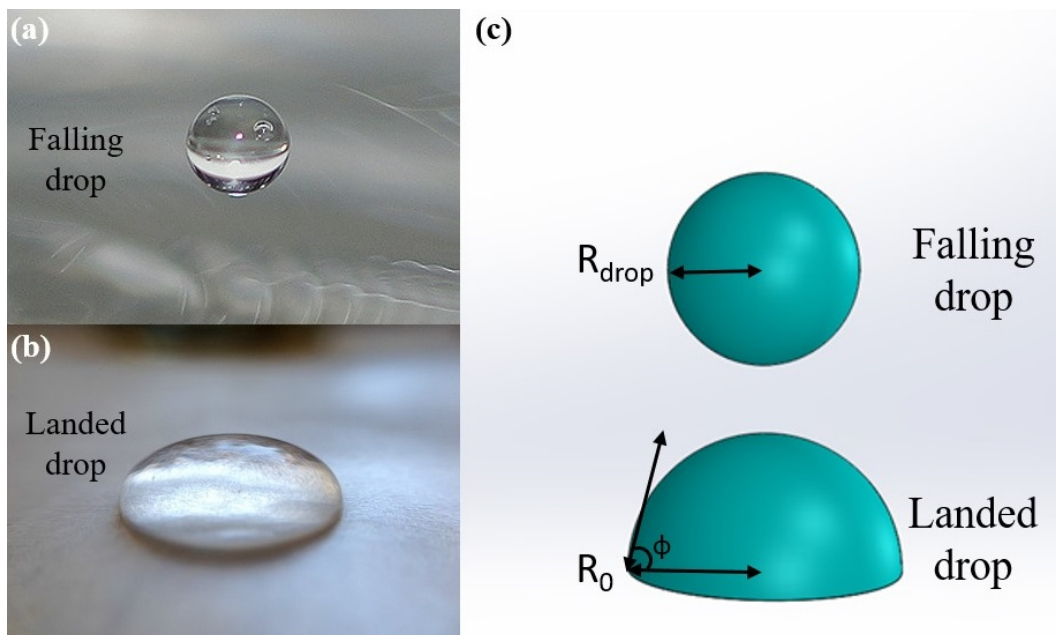


Figure 4.1: Photographs of water droplet (a) suspending in air (b) lying on a solid surface [77] (c) Solidworks drawing of falling and landed drops. Adopted from [78]

In the same manner solids can also be classified according to their some proper-

ties like roughness or smoothness, hydrophobicity or hydrophilicity, chemically homogeneity or heterogeneity, flatness or nonplanarity. Liquid drop dynamics is an important subject in several industrial and environmental situations such as rapid spray cooling of hot surfaces, coating, inkjet printing, quenching of aluminum alloys and steels, rain drop etc. [79].

As can be seen from the Figure 4.1, even though the water droplet suspending in air is in the form of a sphere, it would take a form of spherical cap when it lands to the solid flat surface for minimizing the surface to volume ratio.

## **4.2 Principles of Evaporating Droplets**

### **4.2.1 Surface Tension**

One of the most important questions that can be asked under the scope of this thesis study is why fluids known with their tendency to adopt a shape of their container take a small spherical or hemispherical shapes on some solid flat surfaces instead of spreading out thinly on that surface. This question is explained by the phenomenon of surface tension based on strong intermolecular forces that the liquid-forming molecules exert to each other and these forces are shown by schematic representation in Figure 4.2. While the molecules standing in the middle of the droplet are applied an attractive force in all directions by other molecules in the surrounding, molecules at the surface of the droplet are exerted force just by adjacent molecules in the interior of the drop. That's why interior molecules do not move in a particular direction due to no net force and outer molecules are pushed towards the surface of the droplet due to the absence of external forces which may balance the effect of force caused by internal molecules. As a result of these cohesive forces, water droplet starts to take a hemispherical shape on the substrate by bending and a tension on the surface is created, which is called as a surface tension [80]. Thanks to that tension, there creates a thin surface film structure on the liquid which makes it difficult to be penetrated into and also thanks to the geometrical shape caused by this tension, minimum possible surface area for a given volume of a droplet would be acquired.

Water Droplet on a Solid Surface

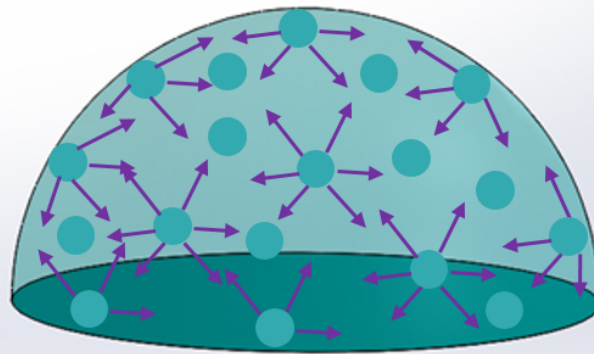


Figure 4.2: Schematic representation of surface tension of a hemispherical water droplet on a solid flat surface. Purple arrows shows the intermolecular forces which molecules apply to each other

Some examples can be given to surface tension phenomenon. For instance, some small insects generally denser than water can walk, float and stride on a water surface due to their inadequate weight to pass through the surface of water. Other example is a water beading on a waxy surface like a leaf. Because of a strong adhesion to itself contrary to weak adhesion to wax, water congregated as a drop. It takes that spherical shape due to the smallest possible surface area for a given volume. Similarly, a paper clip and sewing needle can float on the surface of water.



Figure 4.3: Some examples for surface tension phenomenon (a) water strider on the water surface [81] (b) water beading on a leaf [82] (c) a paper clip in a glass [83]

### 4.2.2 Contact Angle Phenomena and Wetting

Any liquid surface constitute an interface between the liquid and another medium. That's why, it should be considered like that surface tension is not only a characteristic of a liquid but also a property of interface of the liquid with some other medium. The contact angle plays a role of a boundary condition through *Young's Equation* which is used for explanation of balance of forces acting on interfacial tensions, which are solid-liquid, solid-air, and liquid-air, and it is proposed by Thomas Young in 1805 [84]. Demonstration of this phenomenon is shown in Figure 4.4.

Interpretation of this equation can be done shortly in that way. Molecules at the interface have a high potential due to inadequacy of counterparts on the other side of that interface, which gives rise to a force drawing molecules from the interface towards the bulk. So there occurs a potential energy difference transferring into a mechanical work in the liquid system. Contrarily, because the atoms on the solid surface are motionless in terms of the movements from solid to the bulk, situation is slightly different from the state of liquid. There is not a potential difference that can be transferred to mechanical work at the solid-air interface. So, according to this interpretation Young's equation actually does not have a physical foundation in terms of the balance of surface forces. This equation is based on just the surface tensions by neglecting the gravity and additional surface tension caused by the solid surface for providing force balance in the left-side of the equation [85]. Because of that neglect, contact angle calculated theoretically and measured experimentally does not always match with each other.

Another issue that needs to be considered when droplets are mentioned is wetting. When a liquid droplet hits a solid flat surface how does it spread out? Sometimes it overspreads as soon as it strikes to the surface and sometimes beads into several small droplets. It depends on completely the wetting properties of the underlying surface, which can be categorized as hydrophilic, hydrophobic or superhydrophobic. Contact angles are utilized mostly for estimation of surface energy or surface wettability. Also they are the key for surface classification as

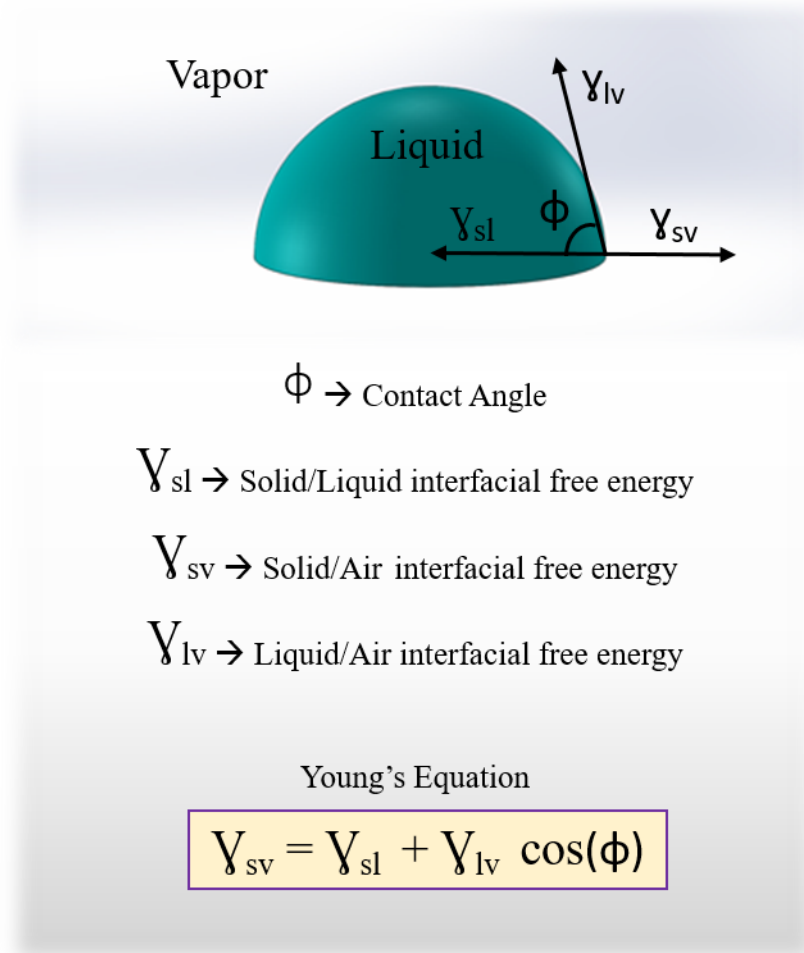


Figure 4.4: Demonstration of the balance of interfacial tensions of a drop lying on a solid flat substrate. In this classical display, there are three mechanical surface tensions in equilibrium in the parallel direction to solid flat surface [86]

hydrophilic or hydrophobic, polar or nonpolar, wetting or nonwetting. While surfaces naturally repelling the water and so allowing droplets to form are called as hydrophobic or water-fearing, surfaces causing droplet to spread and so the contact area to be maximized are named as hydrophilic or water-loving [87]. When the water contact angle is less than  $90^\circ$  then this surface is hydrophilic; this refers to a wetting liquid with low surface tension/low surface energy (see Figure 4.5b). When it is greater than  $90^\circ$ , then the type of surface is hydrophobic and this refers to a non-wetting liquid relative to the surface whose surface energy exceeds that of the solid surface (see Figure 4.5a).

If the angle is even bigger than  $150^\circ$ , then surface is called as superhydrophobic.

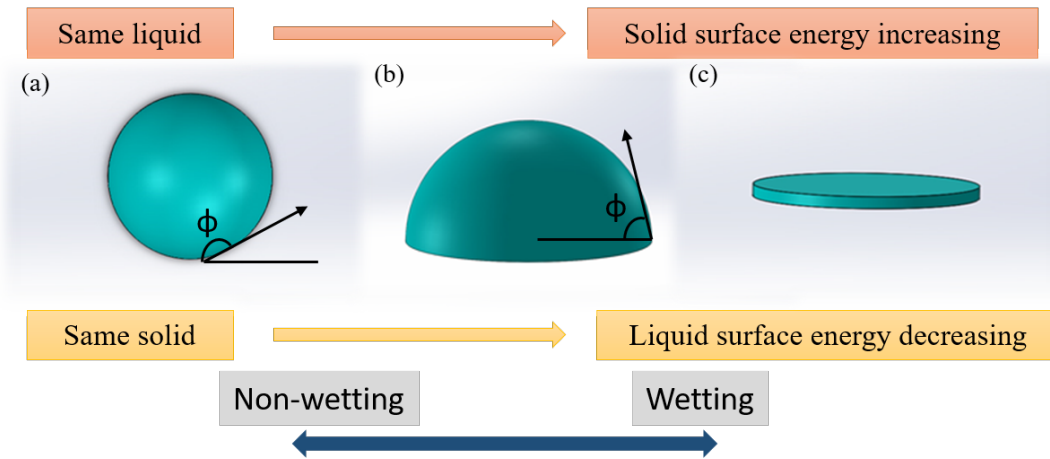


Figure 4.5: Contact angle of a colloidal droplet on a substrate (a)  $\phi > 90^\circ$ , non-wetting, superhydrophobic surface (b)  $\phi < 90^\circ$ , partial wetting, hydrophilic surface (c)  $\phi = 0^\circ$ , complete wetting, superhydrophilic surface

Lastly, when the contact angle equals to  $0^\circ$  and droplets are spread out nearly flat, then the surface is known as superhydrophilic (see Figure 4.5c,4.6). This characteristics of surface can be also improved by changing the shape of the material. For instance, by producing nanopatterns on the surface, contact area of it with the droplet can be enlarged and hydrophobicity of the surface can be amplified to superhydrophobicity, and likewise hydrophilicity property can be amplified to superhydrophilicity [88].

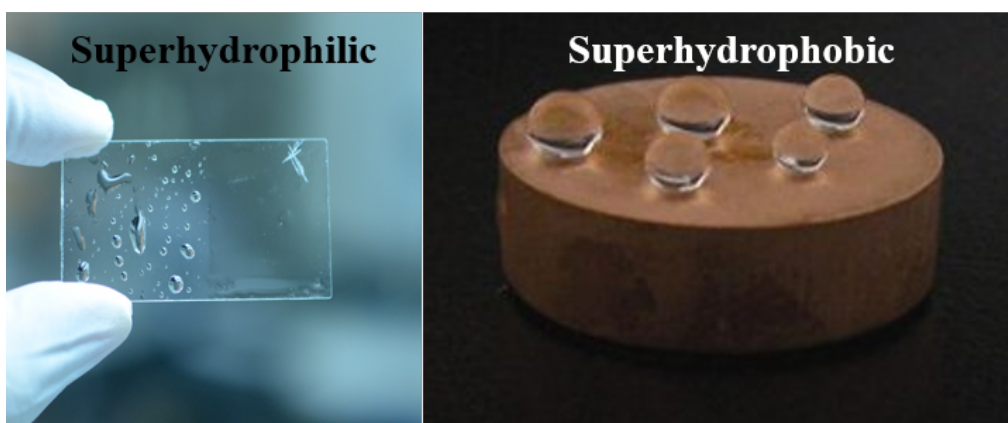


Figure 4.6: Image of water droplets on superhydrophilic and superhydrophobic surfaces [89]

### 4.3 Coffee-Ring Effect

And after mentioning the fundamentals of liquid drops now the order of asking that question: What takes place if the droplet containing dissolved particles is evaporated quickly? It is possible to explain this question by talking about a situation that everybody faces in our daily life. When a spilled drop of coffee dries on a solid surface, the edge of that drop leaves a darker ring-like deposit than the center of the droplet (see Figure 4.7). A drop initially spreading over a large surface concentrate on a smaller area along the perimeter. In the same sense, when a drop of any colloidal suspension pinned on a substrate evaporates, it leaves a dense ring-like deposit at the edge of the droplet. So, that phenomenon is known as “*Coffee-Ring Effect*”. In the light of these explanations, demonstration of evaporation process of colloidal droplet on a solid surface can be seen from the Figure 4.8.

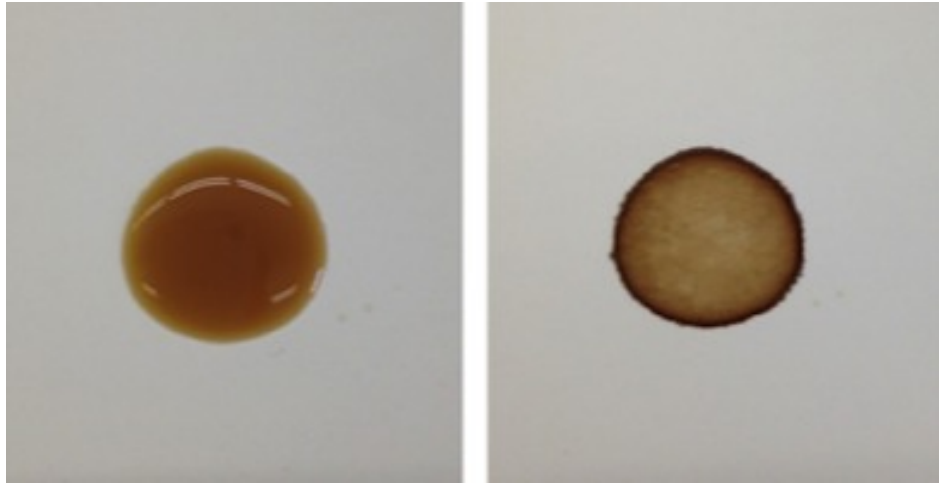


Figure 4.7: Photograph of spilled coffee stains [1]

As can be seen from the Figure 4.8, throughout the drying process of any droplet containing colloidal particles, with the evaporation edges of the droplet become pinned to a solid surface and with the effect of capillary flow happening outward from the center of droplet suspended particles move through the edges and accumulate there. At the end of the evaporation what we have is ring-like deposition constituted with suspended particles highly concentrated along the original drop edge, known as coffee-ring effect.

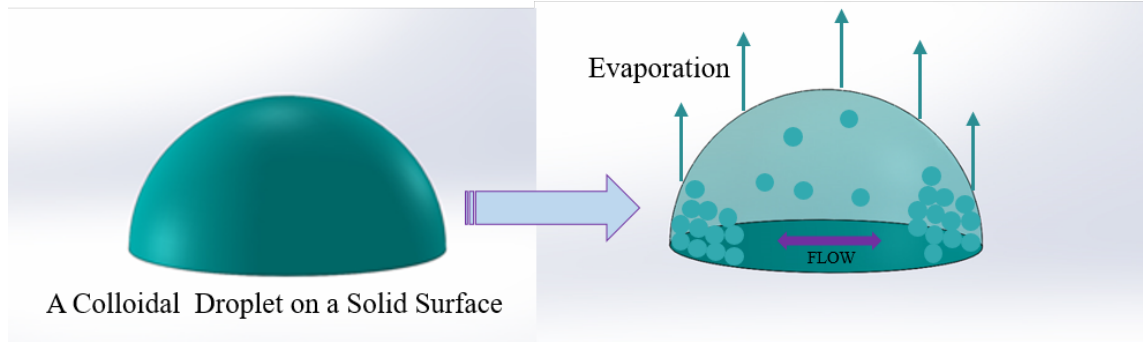


Figure 4.8: Demonstration of evaporation process of colloidal droplet falling on solid flat surface

There are several kinds of dry deposition patterns happening after the evaporation of colloidal droplets. Self-organization of particles suspended in the liquid defines these evaporation-induced formation of patterns [90]. Flow dynamics occurring during the evaporation of the droplet and phase transition cause complex pattern formation such as ring structures [91, 92, 93], fractals [94, 95] etc.

#### 4.4 Applications for Suppression of Coffee-Ring Effect

Controlling the coffee-ring effect and obtaining uniform depositions are very important issue in many applications where particle-containing droplets start drying such as ink-jet printing and coating. To control and even overcome this effect some methods produced and used by many researchers are mentioned in the literature. Let's explain with a few examples.

One of the methods used to achieve homogeneous deposition demand came by Liying Cui and her co-workers is addition of hydrosoluble polymer during droplet evaporation. Because of the viscosity and Marangoni effect, which is a flow resulting from an imbalance of forces with the effect of varying surface tension along an interface, caused by the polymer additives, contact line (CL) of the colloidal droplet moves. Due to the viscosity a great resistance to outward flow is obtained, which causes a deposition containing a small amount of particles at the edge of droplet. Also because of the Marangoni effect, during the evaporation of the droplet containing polymer additives the motion of contact line

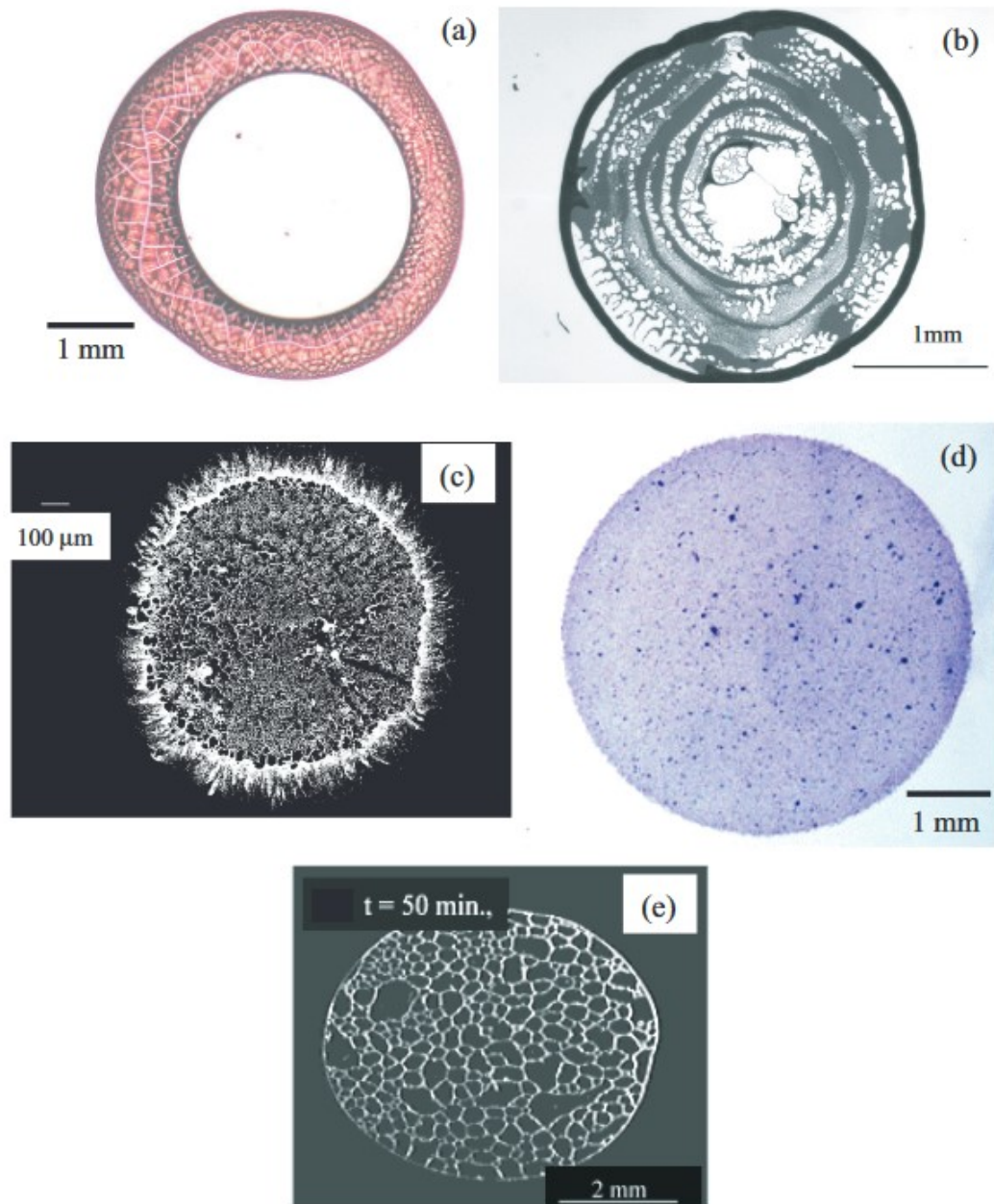


Figure 4.9: Dry deposits in different patterns as a result of evaporation of colloidal droplets (a) ring-like pattern including polystyrene particles (PS) on titanium substrate [96] (b) multiple rings containing PS particles on glass [97] (c) fingering at wetting line with the evaporation of a mixture drop of isopropanol and PS particles on glass [97] (d) uniform deposition pattern with hydroxyapatite particles on titanium substrate [98] (e) hexagonal cells with the evaporation of PS particles on hydrophobic OTS substrate [99]

occurs. Therefore, uniform deposition of  $SiO_2$  microspheres is obtained as can be seen in the Figure 4.10. So, the result extracted from here is that with the

addition of different hydrosoluble polymers the coffee-ring effect can be controlled and even eliminated. This method serves for extensive applications of droplet depositions in biochemical assays, material deposition, photonic devices, sensor array and high-resolution inkjet printing without modification of particle or solvent chemistry [13].

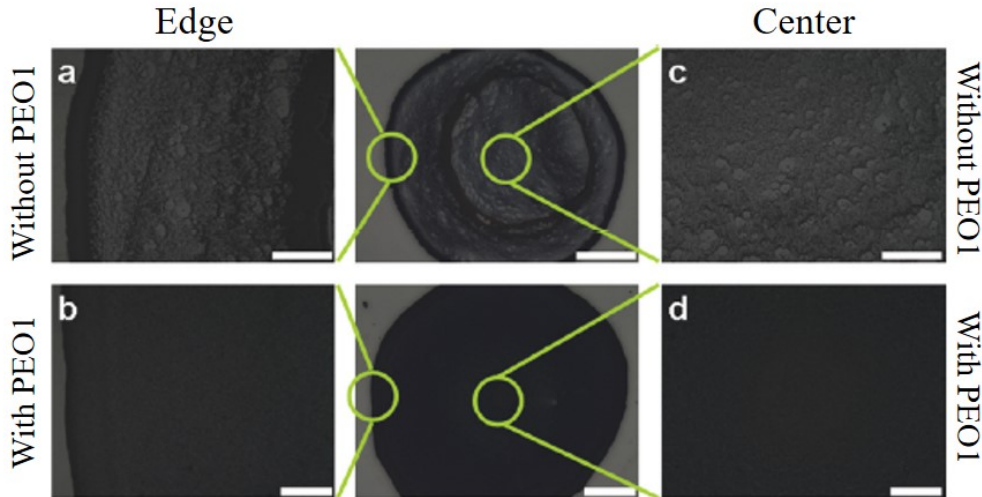


Figure 4.10: Suppression of coffee-ring effect by hydrosoluble polymer additive (PEO1-polyethyleneoxide) for a drop containing  $SiO_2$  microspheres (a,c) without PEO1 (b,d) with PEO1 (a,b) images at the droplet edge (c,d) images at droplet center. Adopted from [13]

Yunker and his colleagues have proposed another method based on shape dependent capillary interactions for suppression of coffee-ring effect. When anisotropic shape of particles are used, in this study it is ellipsoid, it has been observed that deformations such as arrested structures occur noticeably in the air-water interface because of strong long-ranged interparticle attractions between ellipsoidal particles. As a result of these structural deformations of the droplet, suspended particles are prevented from moving towards the edge of the droplet. This allows the coffee-ring effect to be controlled and uniform deposition is formed. Similarly, when the suspension of spherical particles mixes with a small amount of ellipsoidal particles, it is seen that again uniform deposition is obtained. So, the result that can be said by looking at this work is that deposition of particles and therefore the coffee-ring effect can be controlled by also shape of the suspended particles without modification of particle or solvent chemistry [19]. Experimental evidence of this study can be seen in Figure 4.11.

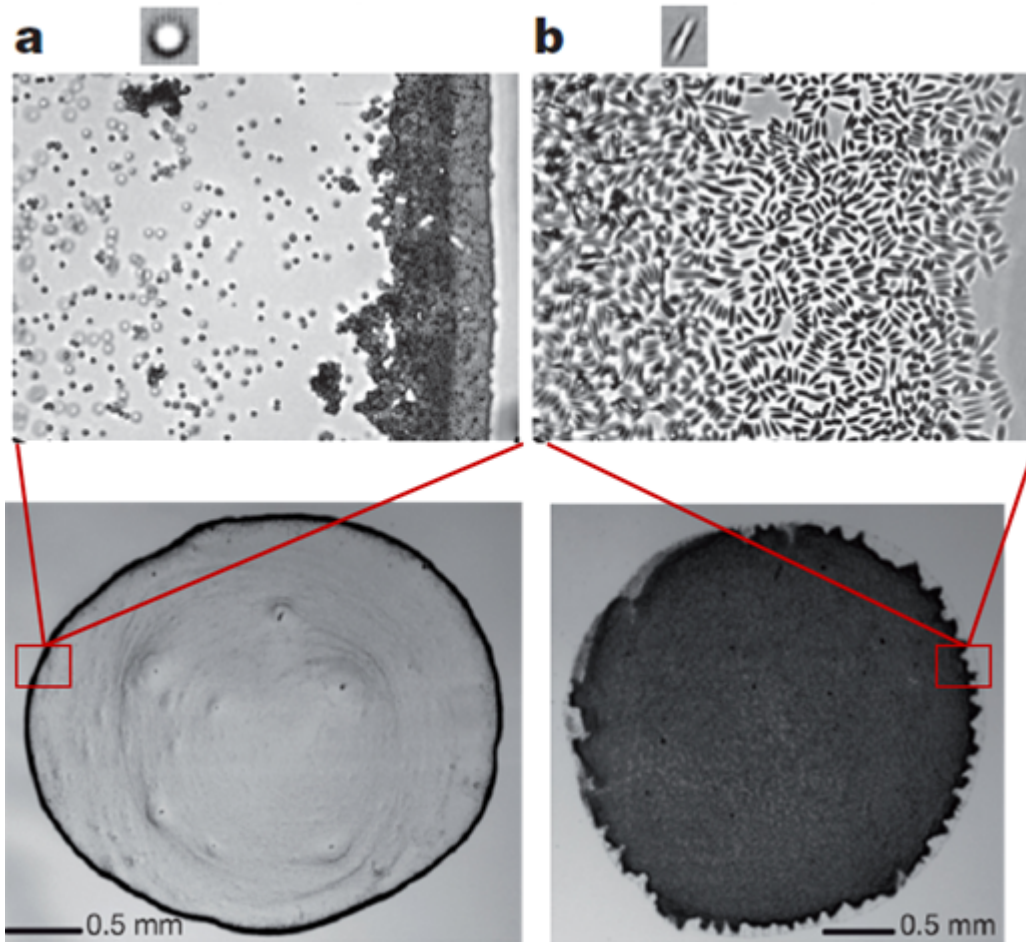


Figure 4.11: Suppression of coffee-ring effect by shape-dependent capillary interactions (a) suspension of spherical particles (b) suspension of ellipsoidal particles. Adopted from [19]

In seeking a simple and more general solution to obtaining homogeneous disc-like or concentrated spot-like residues, another potentially useful method in an extensive range of industrial and analytical applications where homogeneous solute depositions are desired to be used is acoustic suppression of coffee-ring effect without any necessity of physiochemical modification of the fluids, the particles or the surface [20].

With an interaction between surface acoustic waves and the droplet containing polystyrene particles, at the nodal points of stationary waves producing patterns the particles are trapped. Particles do not move towards the contact line with the capillary flow formed by evaporation in consequence of a trapping of them within the patterns. Because of the free of particle depositions in the contact

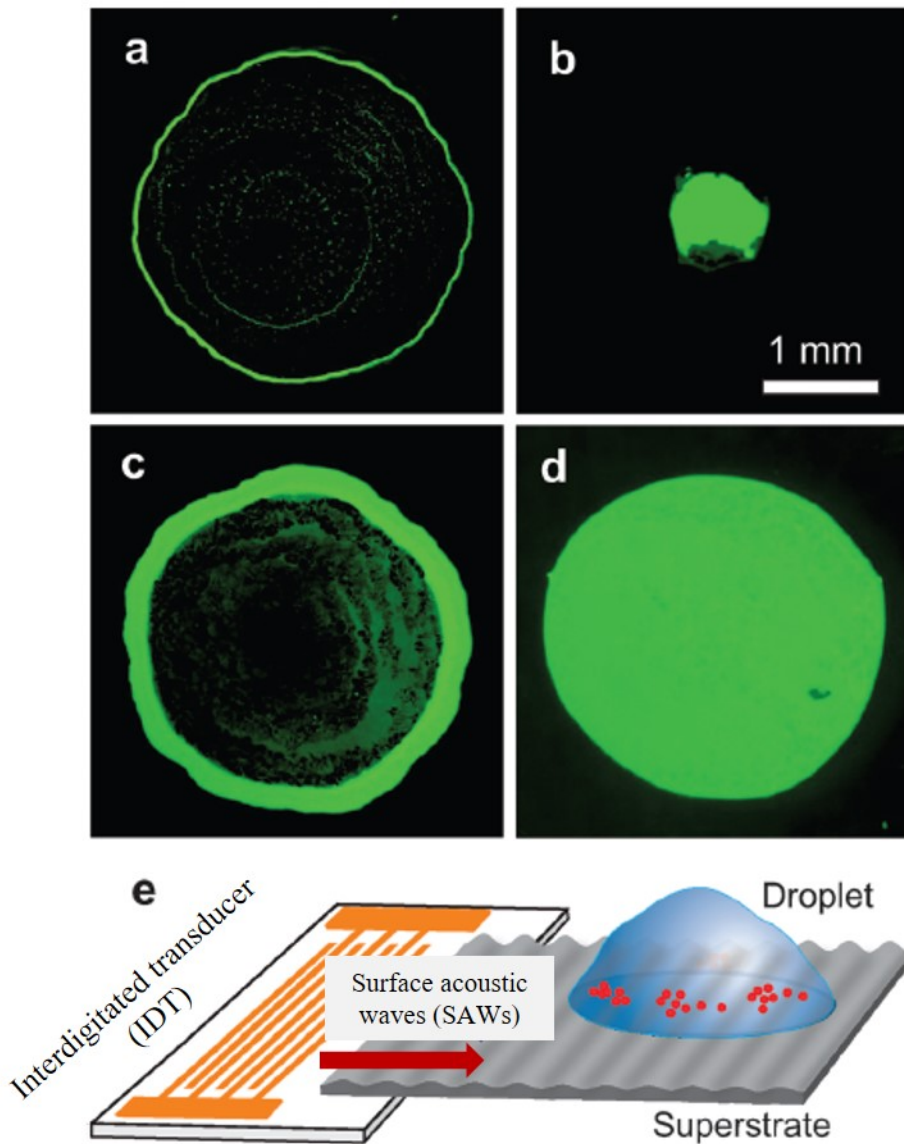


Figure 4.12: Suppression of coffee-ring effect by acoustic waves. Fluorescent images of residues for  $2\mu\text{l}$  water droplet containing  $2\mu\text{m}$  polystyrene (PS) particles (a,c) without surface acoustic waves (b,d) with the application of surface acoustic waves (a,b) lower volume fraction (0.1%) (b) 9.7MHz frequency (c,d) higher volume fraction (2.5%) (d) 20MHz frequency. Adopted from [20]

line, that line recedes freely and there happens a concentrated spot-like residue with the convergence of trapped particles. So, the coffee-ring effect is suppressed with the help of surface acoustic waves. Also, the size of the residue can be adjusted depending on the particle concentration in the droplet. It increases in direct proportion to the concentration. Experimental evidence of this study can be seen in Figure 4.12.

After examining the methods given above by a few important examples, we wanted to test and develop a new method that makes up the subject of this thesis in order to control and even overcome the coffee-ring effect. We aimed to observe the same effect under optical potential. Have we succeeded in suppressing the coffee-ring effect under the random optical potentials or not? The experimental steps, experimental setup, results obtained and interpretations are included in the next chapter. Let's see the answer then.



## CHAPTER 5

### EXPERIMENTAL RESULTS

#### 5.1 Introduction

After a while over the drying of the coffee drops on a solid surface such as a table, wall or dish in daily life, we would see some ring-like coffee residues known as “coffee-ring” effect first proposed by Deegan in 1997 [100]. This phenomenon occurs with the combination of two different effect:

- The state of fixation, which means “pinning/depinning”, of drop’s contact line on the solid substrate.
- The convective evaporative flux that pushes the suspended particles in the liquid droplet towards the edge boundaries (contact line) by radial flow.

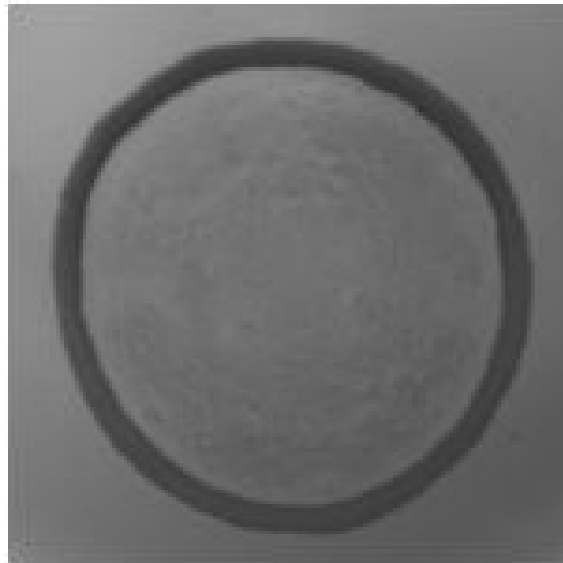


Figure 5.1: Full view of the droplet after evaporation

In many applications, this ring-like heterogeneous residue is something to be avoided due to the need to obtain uniform material deposition across the whole surface. That's why, the coffee-ring effect is a long-standing and significant issue for many applications such as inkjet printing. In order to suppress the coffee-ring effect and to obtain disk-like homogeneous patterns, numerous studies on evaporation induced patterning of a drop consisting of nonvolatile solute (such as nanospheres, nanoparticles, polymers, DNA, etc.) and volatile solvent have been performed. Until now, all studies done to eliminate this effect have taken place around two cases, which are mentioned above. One is to prevent the pinning of drop's contact line, and the other one is to prevent the deposition of suspended particles near the contact line.

Here, in this work, we investigate the evaporation of liquid droplets containing passive ( $3\ \mu\text{m}$  polystyrene particles) and active particles ( $3\ \mu\text{m}$  polystyrene particles along with motile *E. Coli* cells) in the presence of a random optical potential generated by a speckle light field.

## 5.2 Materials and Methods

### 5.2.1 Experimental Setup

Observation of the evaporation process of the droplets were made by means of the system designed as shown in Figure 5.1. A home-made inverted microscope was constructed for that purpose. The setup includes a number of optical components on a stabilized optical table so as to avoid the disturbances coming from the environment and to obtain a stable alignment of optical elements because even small vibrations or strain in the table on which the elements are set up might give rise to complete failure of an experiment.

The system contains three different cameras controlled by a computer and their purpose is to observe the full view of the droplet ( $C_1$  in the Figure 5.2), the side view of the droplet ( $C_2$ ) and the magnified view of a fraction of the droplet ( $C_3$ ) respectively by digital video microscopy simultaneously with the help of an incoherent white light (WI) directed on the droplet by beam splitter ( $BS_1$ ) and mirror (M). 4X microscope objective ( $O_1$ ) with the numerical aperture of 0.13

was used for recording the full view. Illuminated light was reflected onto the CMOS camera  $C_1$  by use of beam splitter ( $BS_2$ ) positioned between the lamp and the sample holder (S). Side view was recorded by using 10X microscope objective, numerical aperture (NA) of 0.30 and a convex lens with a focal length of 35.0 mm with a monochrome CCD camera ( $C_2$ ) which were located on XY translation stage so that the accurate position of the droplet could be detected easily. And lastly, for the magnified view of a fraction of the droplet, another microscope objective (20X, NA=0.5) was used with a CCD camera ( $C_3$ ). We need a camera which has high magnification property to be able to study the behavior of suspended particles in the droplet, and when compared to first two cameras, this one makes available a higher magnification. In order to obtain synchronized results throughout the experiments, frame rate of all of these cameras was set to 7 fps.

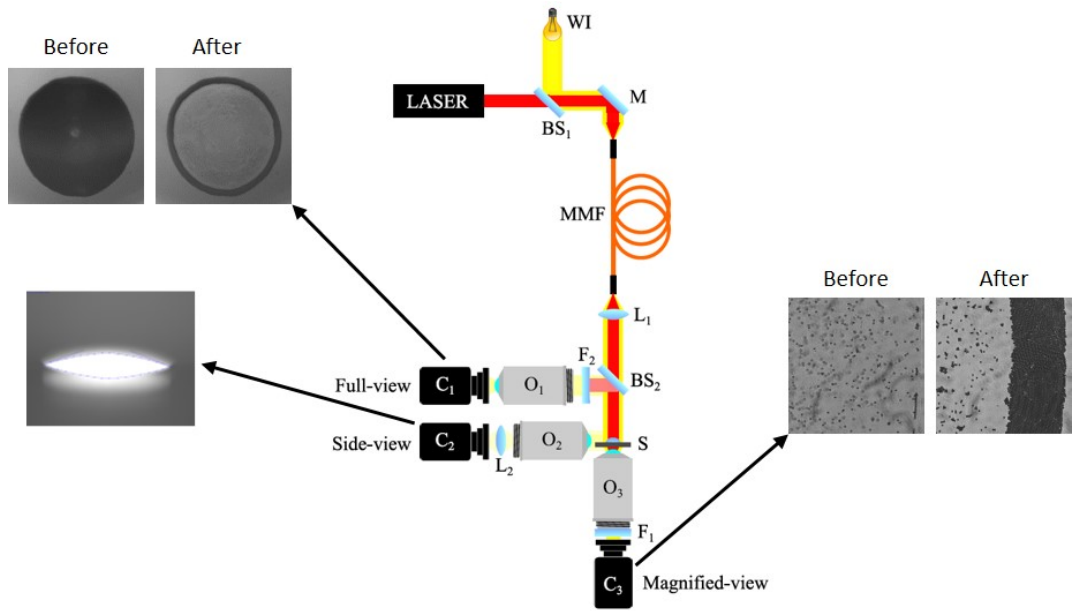


Figure 5.2: Schematic representation of the experimental setup: Home-made inverted microscope capable of recording full view of the droplet, side view of the droplet and magnified view of a fraction of the droplet.

In the speckle optical tweezer setup which is schematically depicted in Figure 5.2, laser beam, which is infrared (IR) in 980 nm wavelength, was coupled into a multimode optical fiber to generate the speckle light pattern for the manipulation of colloidal spheres. Speckles are caused by light propagation in a multimode optical fiber waveguide and the reason obtaining a random appearance of speckle

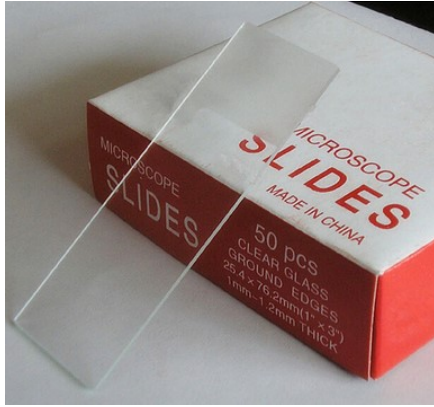
patterns is that because of different eigenvalues of the fiber, large number of optical waves interfere with each other in random phases [73, 101]. There are many ways to generate a speckle pattern like multiple scattering in an optically complex medium, scattering of a laser on a rough surface, mode mixing in a multimode fiber [73]. Here, in our work, we used the last one. Output power of the diode laser was measured 602 mW at most. Measurements were done with & without collimator and it was seen that there is almost no lost. Laser and the incoherent white light coupled into the same fiber and they were directed onto the sample with the help of other optical components such as beam splitters ( $BS_1$  &  $BS_2$ ), mirror (M) and lens ( $L_1$ ).

### 5.2.2 Cleaning Procedure for the Glass Slides

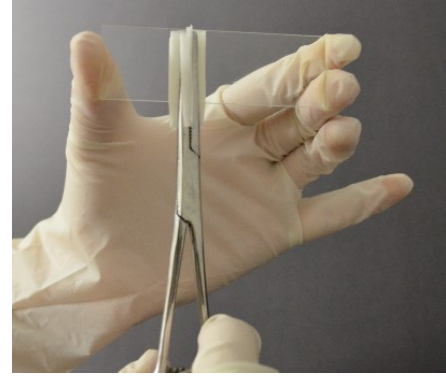
Microscope glass slides (Sail Brand, China) used for that work all through the experiments have 25.4 mm x 76.2 mm (1 in x 3 in) size and 1.0 mm thickness. In order to perform experiments under the same conditions and to obtain the identical surface quality for each microscopic slide, the same cleaning procedure was followed. There are some contamination and impurities on the surface of these slides and before doing the experiments we have to get rid of them. For this purpose, the glass slides were cleaned with first acetone and right after with isopropanol by using a folded lens cleaning tissue by wiping it across from one edge of the slide to the other as can be seen in the Figure 5.3. And then, they were put in the prepared 0.25 M of sodium hydroxide (NaOH) solution. Slides were held for about 1 hour inside that solution. The purpose to make this process is to reduce the adhesion of the particles onto the microscopic glass slides and to make their surfaces hydrophilic.

### 5.2.3 Sample Preparation

Experiments were conducted by using the polystyrene (PS) particles, which its diameter is 3.00  $\mu\text{m}$ . Samples were prepared as two different colloidal suspensions. One contains passive (3- $\mu\text{m}$  monodisperse spherical polystyrene) particles and the other one includes active particles (3- $\mu\text{m}$  polystyrene particles along with motile *E. Coli* cells) with the volume fraction  $\phi=0.001$ . For the sample



(a) Microscope Glass Slides



(b) Cleaning the slide with lens cleaning tissue

Figure 5.3: Cleaning Procedure

containing passive particles, sample content is  $29 \mu\text{l}$  of monodisperse spherical polystyrene particles (Micro particles GmbH, Berlin, diameter  $d = 3.00 \pm 0.07 \mu\text{m}$ ) and  $971 \mu\text{l}$  deionized water. On the other hand, the other sample is prepared with  $29 \mu\text{l}$  of monodisperse spherical polystyrene particles and  $971 \mu\text{l}$  of motility buffer consisting of *E. Coli* separately.

### 5.2.3.1 Preparation of the Motility Buffer and Bacteria Culture

The way of preparing the bacteria we have applied in our laboratory, which is a kind of RP437 (*E. Coli* Genetic Stock Center, Yale University) cell culturing protocol, is like the following respectively. The bacteria is inoculated in 50 ml of Tryptone Broth (TB) inside a 250 ml flask overnight, which is typically 17 hours at  $32^\circ\text{C}$  and 180 rpm in a shaker incubator. After the saturation has been completed, that prepared culture is diluted 1:100 into a 50 ml of fresh medium of Tryptone Broth (TB), which is a growth medium for bacteria, inside another 250 ml flask. Then, under the identical conditions, this diluted culture is incubated for an extra 4 hours and 10 minutes with the overnight culture incubation until its optical density at 600 nm, which means OD600, reaches to 0.4. Into two falcon tubes, 7 ml of the diluted culture is placed and centrifuged at 2000 rpm (for up to 10 minutes at room temperature). After centrifugation process is complete, RP437 cell pellets precipitated at the bottom of the falcon tube is mildly collected by means of pipette. It can be thought of as harvest time. Then, the resultant pellets is suspended again in 5 ml of motility buffer.

The ingredients of this motility buffer is as follows:

- 10 mM of Potassium Phosphate (Monobasic)
- 0.1 mM of Na - EDTA (Ethylenediamineteraacetic acid) (pH 7.0)
- 10 mM of Dextrose (D-Glucose ( $C_6H_{12}O_6$ ))
- 0.002 % Tween 20—2  $\mu$ L for 100 mL of deionized water

The washing procedure, which is centrifugation, harvesting and suspending of the bacteria in the motility buffer, is repeated three times so that it is possible to get rid of the growth medium to the extent possible.

#### 5.2.4 Experimental Procedure

Several trial experiments were conducted to determine the experimental parameters before starting to obtain final results. These parameters are particle concentration rate, cleaning procedure for microscopic slides (with NaOH or without NaOH, and for slides, soak time in NaOH solution), particle size, drop size, evaporation rate (fast and slow evaporation, which is possible to cover slide with another slide channeled with parafilm).

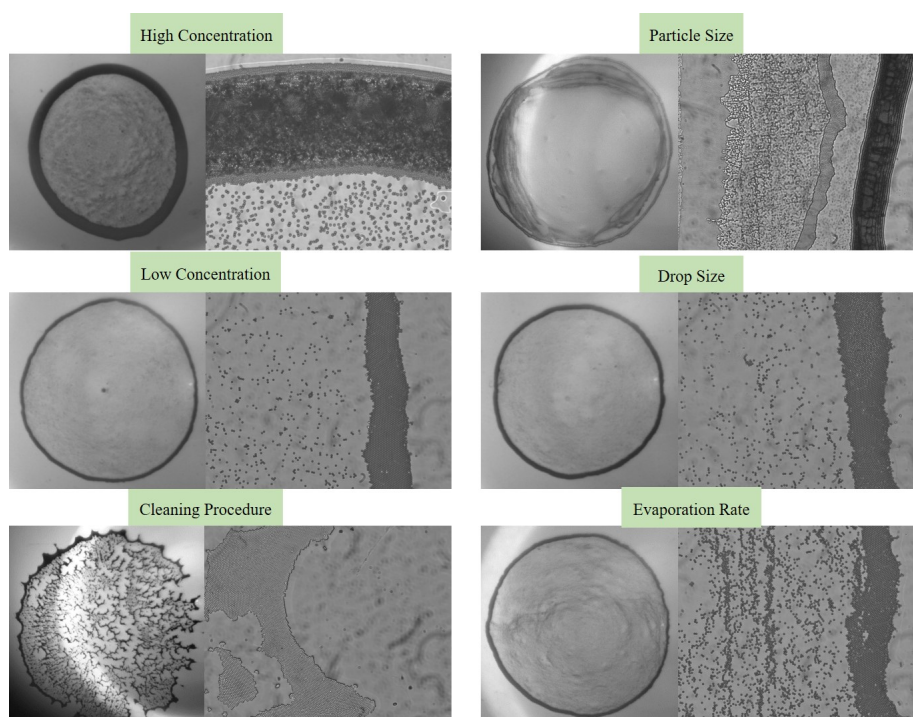


Figure 5.4: Experiment parameters tried before starting to take main results

## 5.3 Results without Optical Potential

### 5.3.1 Droplets Containing Only Passive Colloidal Particles

3  $\mu\text{l}$  of deionized water droplet consisting of 3  $\mu\text{m}$  polystyrene particles was dropped on the microscope slide, which was previously held for about 1 hour inside 0.25 M of sodium hydroxide (NaOH) solution prepared by me for making the surface of slide hydrophilic. When a drop of polystyrene particle (3  $\mu\text{m}$ ) suspension evaporates on a solid surface, we observed that the suspended particles tend to kinetically accumulate at the air-liquid interface and it commonly leaves a ring-like deposit along the edges, known as coffee-ring phenomenon. Figure 5.5 shows the accumulation of particles at the contact line as a function of time forming a coffee-ring.

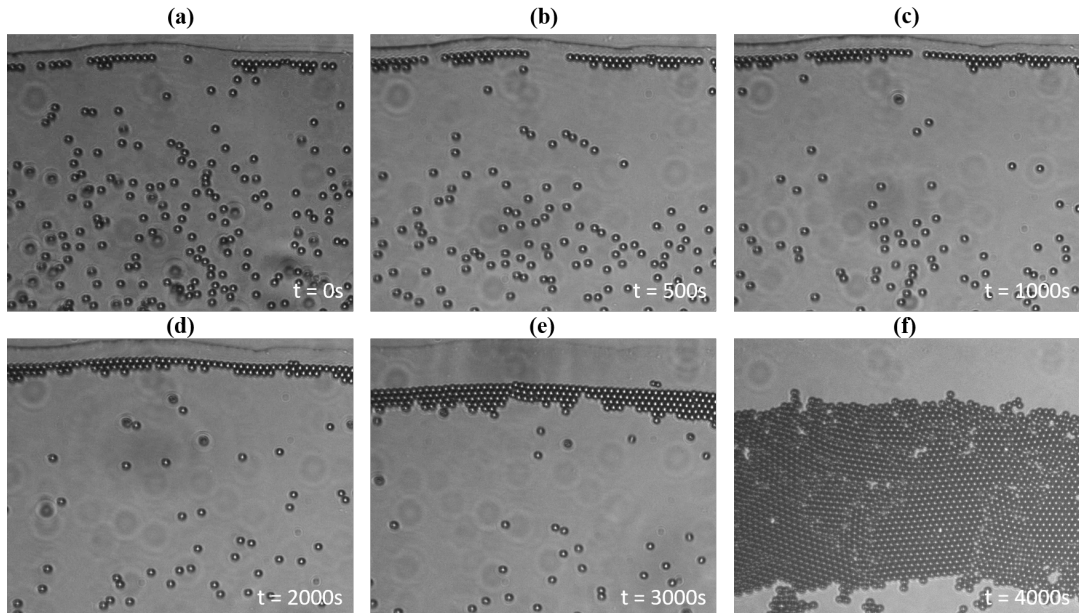


Figure 5.5: Edge images of deionized water droplet consisting of 3  $\mu\text{m}$  polystyrene particles. From (a) to (f) the change in particle movements over a period of 4000 seconds is shown.

### 5.3.2 Droplet Containing Passive Colloidal Particles along with Active Particles

When a drop containing polystyrene particles (3  $\mu\text{m}$ ) together with bacteria (motile *E. Coli* cells) evaporates on a solid surface, again a similar coffee-ring

effect was observed. However, when compared to previous figure, which is Figure 5.5, the accumulation of particles is limited because of the activity of the *E. Coli* cells. Due to this reason, not all the particles accumulate at the contact line. Importantly, the information obtained from this experiment is that the dynamics of active particles are different from those of passive particles.

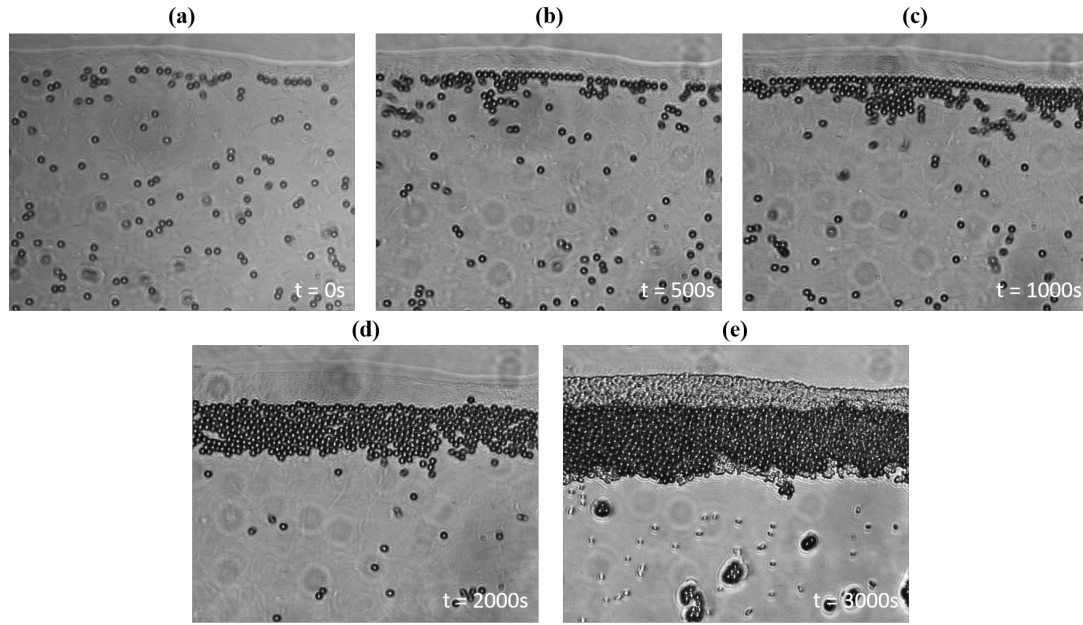


Figure 5.6: Edge images of deionized water droplet consisting of  $3 \mu\text{m}$  polystyrene particles and bacteria (motile *E. Coli* cells). From (a) to (e) the change in particle movements over a period of 3000 seconds is shown.

## 5.4 Results with Optical Potential

### 5.4.1 Droplets Containing Only Passive Colloidal Particles

In the second part of our work, unlike the first part, the laser was integrated into the experimental setup and experiments continued in this way to observe the effect of laser on suspended particles' motion. Then, it is observed that under the influence of a random optical potential (Power=50mW), the optical forces trap the passive particles meta-stably and therefore, the suspended particles are prevented to reach the drop edge (see Figure 5.6) forming uniform deposition (see Figure 5.8).

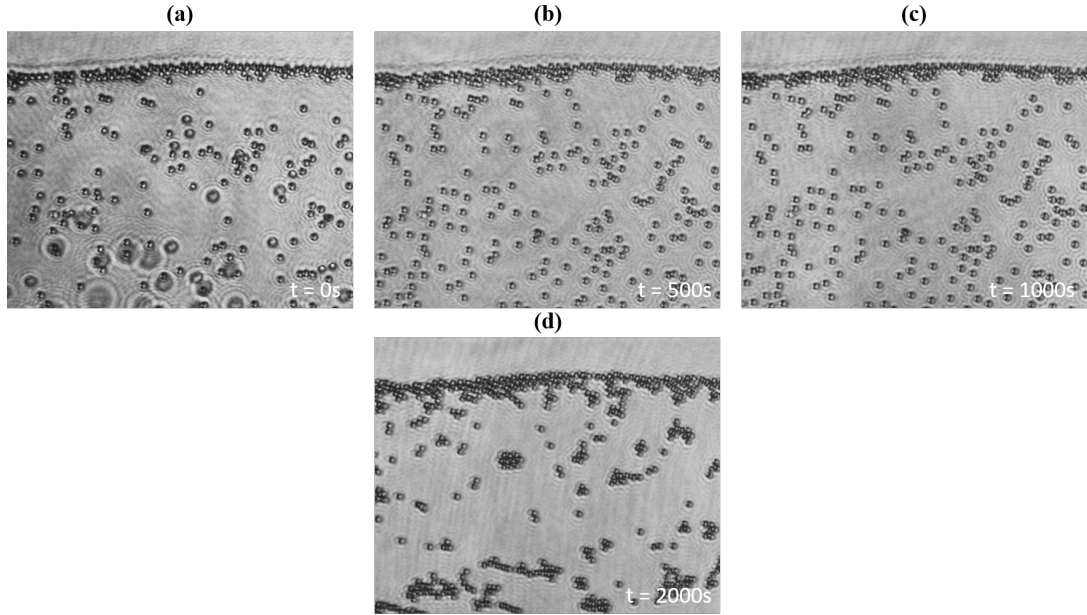


Figure 5.7: Edge images of deionized water droplet consisting of  $3 \mu\text{m}$  polystyrene particles. From (a) to (d) the change in particle movements over a period of 2000 seconds is shown.

#### 5.4.2 Droplet Containing Passive Colloidal Particles along with Active Particles

In this section, we observed changes under random optical potential in the droplets obtained by adding active particles that we produced in our laboratory, which is RP437 bacterial cells (motile bacteria *E. Coli* cells), in addition to passive colloidal polystyrene particles. Consequently, observations are as follows:

- 1) The random optical potential meta-stably trap the particles and
- 2) the presence of bacterial activity additionally prevents the particles from reaching the contact line.

Results obtained in this part can be seen in Figure 5.8.

### 5.5 Comparison of the Results and Discussion

Image of a drop containing polystyrene particles is shown in Figure 5.9. It is easily seen that under the influence of a random optical potential the coffee-ring

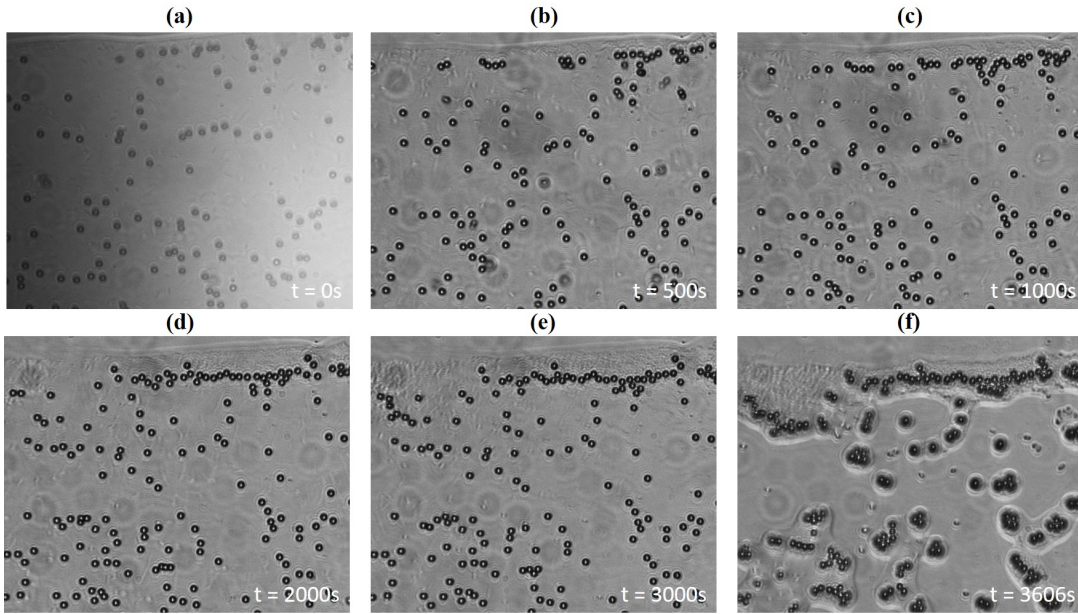


Figure 5.8: Edge images of deionized water droplet consisting of  $3 \mu\text{m}$  polystyrene particles and bacteria (motile *E. Coli* cells). From (a) to (f) the change in particle movements over a period of 3606 seconds is shown.

effect disappears and uniform deposition occurs.

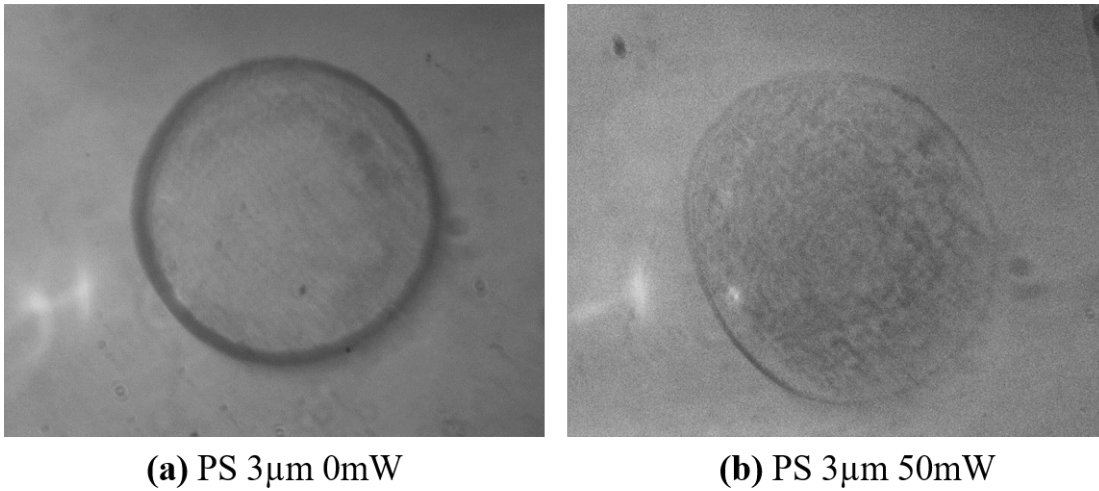


Figure 5.9: Full images of deionized water droplet containing  $3 \mu\text{m}$  polystyrene particles. (a) and (b) shows the change in particle movements during the all evaporation process.

Image of a drop containing polystyrene particles and bacteria is shown in Figure 5.10. It is easily seen that under the influence of a random optical potential again the coffee-ring effect disappears and uniform deposition occurs.

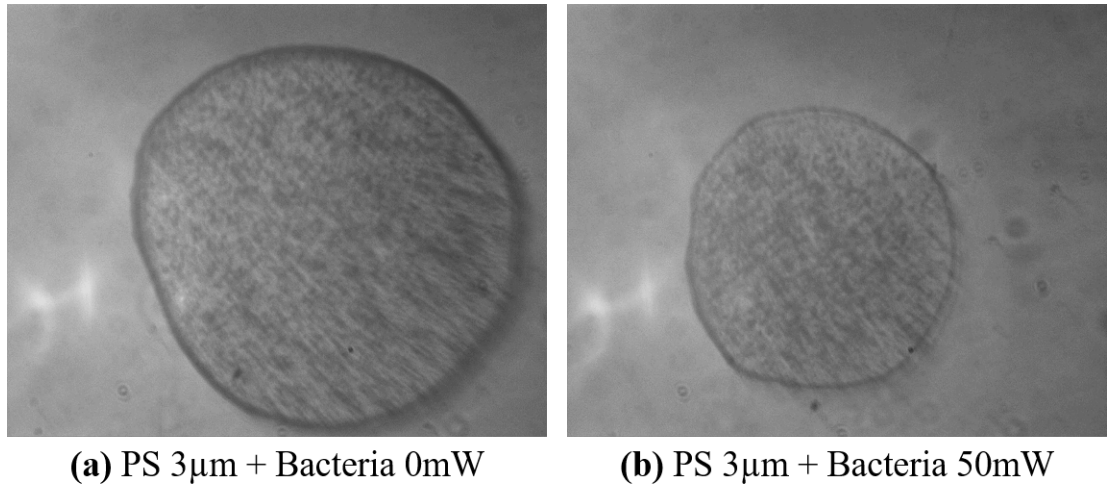


Figure 5.10: Full images of deionized water droplet containing 3  $\mu\text{m}$  polystyrene particles and bacteria (motile *E. Coli* cells). (a) and (b) shows the change in particle movements during the all evaporation process.

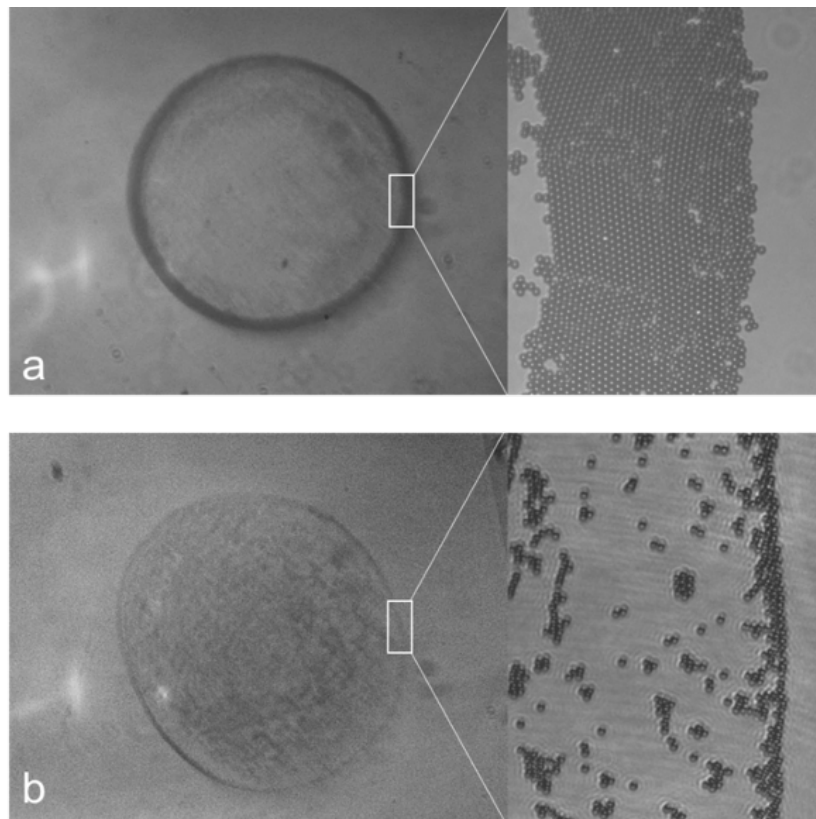


Figure 5.11: When no optical potential is applied (a) the passive particles tend to migrate towards the rim of the drop exhibiting the coffee-ring effect. The coffee-ring effect is suppressed when a random optical potential is applied over the drop (b).

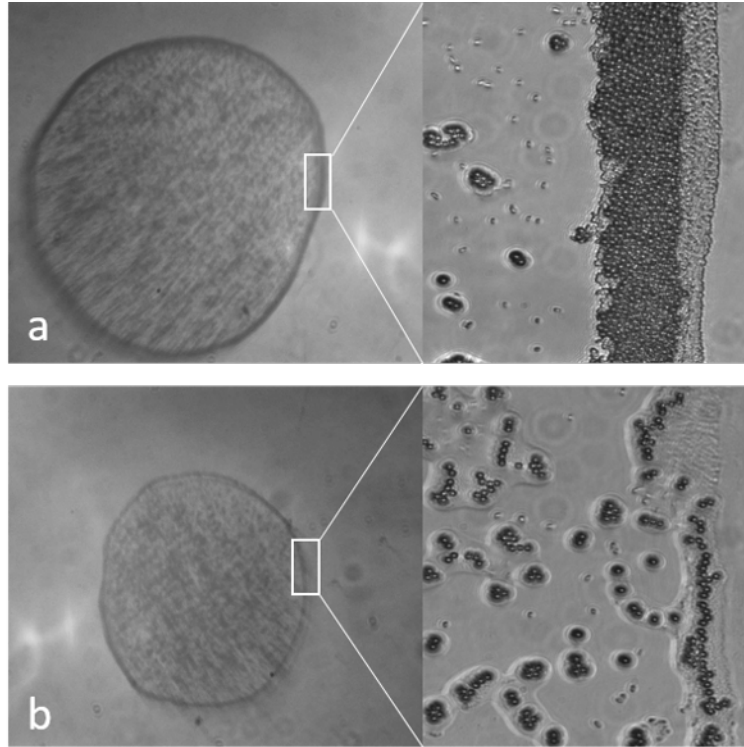


Figure 5.12: When no optical potential is applied (a) the similar particles in active bath tend to accumulate at the air-liquid interface. The coffee-ring effect is completely suppressed when a random optical potential is applied over the drop area (b).

When we compare all these images of drying droplets containing active (*E.Coli* cells) and passive (polystyrene-PS) particles with the successful results obtained with other different techniques that have gone through the literature, we see that this method, which has been considered and applied for the first time, has become an alternative method that can be used to solve the coffee-ring effect problem. Comparative knowledge can be obtained from Figure 5.13. Another result that we can make an inference by looking at these images is that even though all these methods have been successful in suppressing the coffee-ring effect and achieving a homogeneous disk-like distribution instead of a nonuniform ring-like deposit, a small amount of droplet contact line is still detected after the evaporation process as in the method applied in this thesis. It can be seen easily with red ellipsoids in the images below. So, it is not right to say that this is a failed method since the coffee-ring effect is largely suppressed and a homogeneous disk-like residue is obtained.

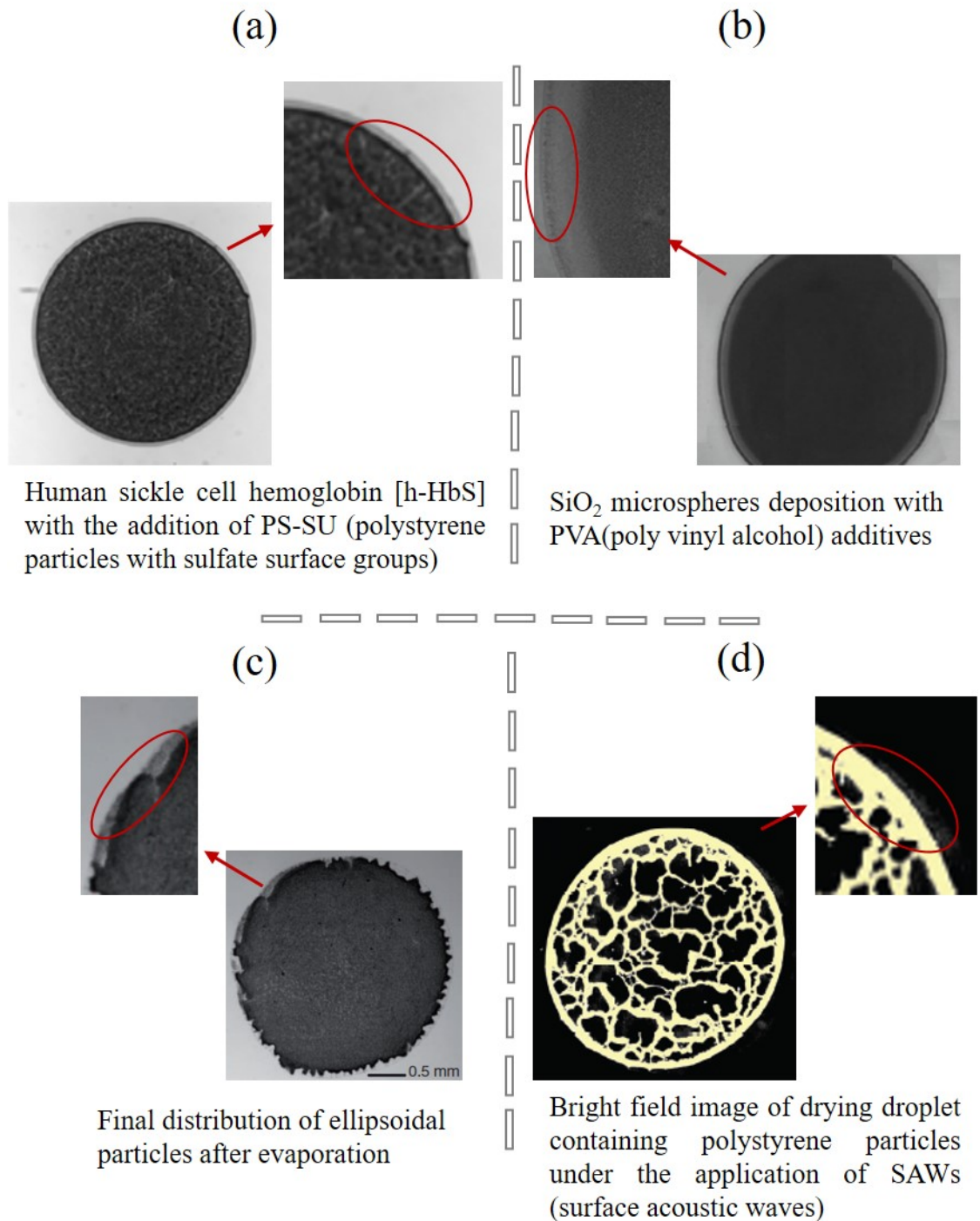


Figure 5.13: Comparison of results obtained with different techniques for the suppression of coffee-ring effect [102, 13, 19, 20]

To be able to suppress or overcome the coffee-ring effect, it is required to control the strength of Marangoni or Capillary flow, and it is possible with the change of some factors including substrate temperature, suspended particle size and

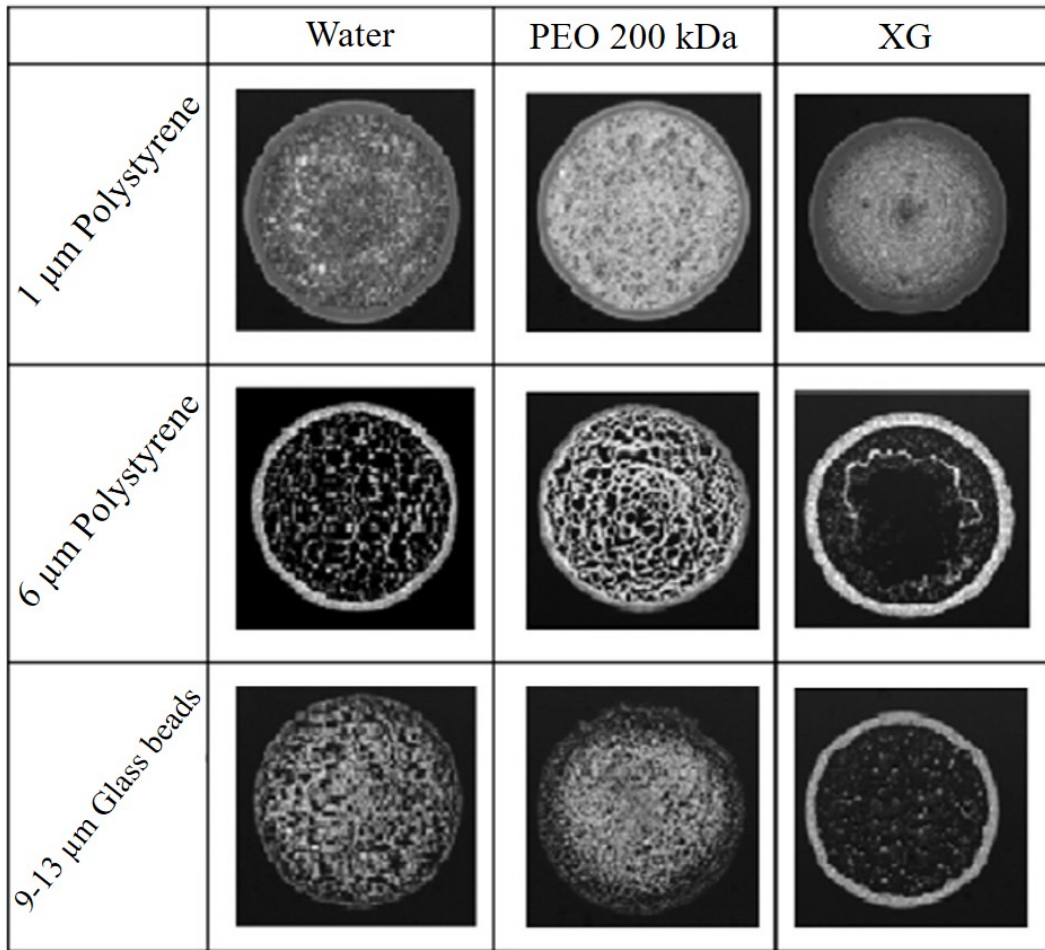


Figure 5.14: Effect of three different kind of solvents on coffee-ring effect [103]

solvent type. The solvent environment of all of the droplets in the experiments in this thesis is water. However, the effect of different solvent environments on the coffee-ring effect has also been observed and is included in the literature. The effect of three different kind of solvents, which are pure water, polyethylene oxide (PEO) and xanthan gum (XG), on coffee-ring effect is shown in Figure 5.14. It is observed here that a droplet containing any suspended particle may exhibit different behaviors in different kind of solvent environments because every fluid has a different viscosity and viscosity properties of fluids affect the Capillary flow and thus the motion of suspended particles. For example, while larger particles suspended in the XG solution form a ring-like coffee stain pattern, the ones suspended in the water and PEO solution formed a more homogeneous disk-like pattern. In this thesis, experiments were only conducted in water environment and was successful. At the next stage of the study, experiments can be performed

in different solvent environments and different size of suspended particles, and it can be observed whether the optical potential application for the suppression of coffee-ring effect will be successful in changing conditions or not.

In addition to experimental studies mentioned so far, some theoretical studies on this subject have been also made and mathematical models have been developed. One of them is a Monte Carlo model, which uses the diffusion-limited aggregation (DLA) approach coupled with the concept of the biased random walk (BRW) for simulation the particle migration and agglomeration throughout the evaporation process of droplet, is developed to examine the transition from the coffee-ring deposition to the homogeneous disk-like deposit in drying colloidal droplets. Thanks to that mathematical model, the importance of the simultaneous presence of the particle adsorption, long-range attraction and circulatory motion processes is shown.

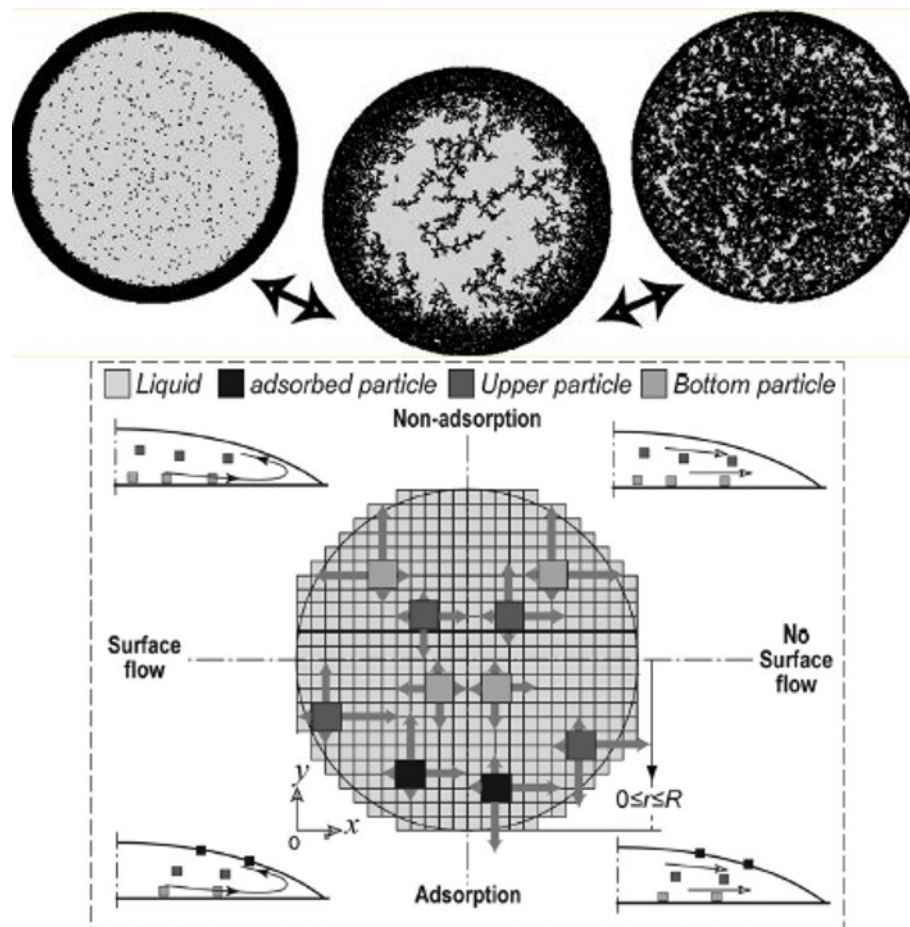


Figure 5.15: Schematics of the simulation process. [104]

Another alternative mechanism for coffee-ring deposition is a theoretical model, which has the Eulerian and Lagrangian forms. With the Eulerian description of model, it has shown that the alteration of the form of evaporative flux to have a uniform deposition patterns enables to control the shape of coffee-ring deposition pattern. Evaporation of sessile droplets on both hydrophilic and hydrophobic surfaces, which results in either diffusive or uniform over the surface, has examined and coffee-ring deposition patterns has investigated by using this theoretical model. [105]

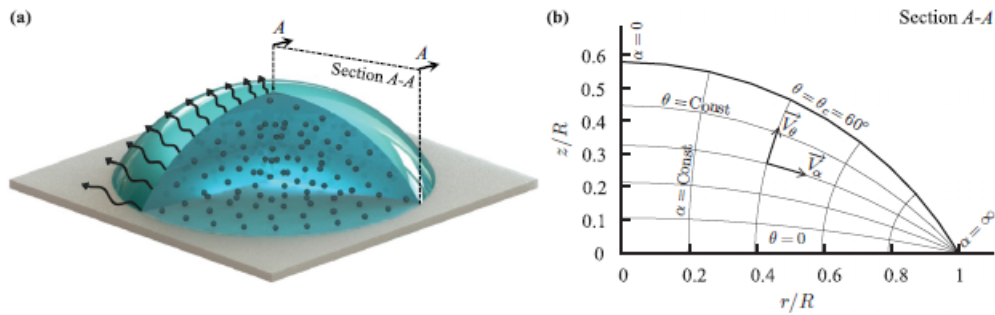


Figure 5.16: A colloidal droplet evaporating on a flat substrate. (a) droplet consisting of nonvolatile particles (b)  $\alpha$ ,  $\theta$  and velocity components are shown in a toroidal coordinate system and they fits the contact line of the droplet on the meridian plane A-A. [105]

Based upon these theoretical models explained above, for the method described throughout this thesis, which is the "suppression of coffee-ring effect in random optical potentials", it may be possible to create some mathematical models in future studies.

## CHAPTER 6

### CONCLUSION

It is possible to observe the random movement of particles in fluids such as air, oil or water, which happens as a result of their collisions with other molecules or atoms, in numerous natural phenomena ranging from the mobility of organelles within a biological cell and the diffusion of calcium through bones to movement of “holes” electrical charge in semiconductors and to even the diffusion of stars within a galaxy. This random motion called as Brownian Motion has a great importance in terms of the wide use of many different areas such as physics, chemistry, biology, engineering, economics and mathematics. All molecules and all colloids in the suspension do this never ending motion at the micro-scale. When we want to study these systems, this motion makes it very hard to do so. That’s why, we have the need to confine their motion.

Coffee ring phenomenon first proposed by Deegan in 1997 [100] was found that because of the accumulation of suspended solutes (for example, colloidal particles) at the contact line of air-liquid interface as a result of a larger evaporative flux towards the edge, there occurs a ring-like residue. For several applications, we need to control the mechanism of this phenomenon to prevent this occurrence and to obtain a disc-like homogeneous structure instead of a ring-like non-uniform structure. Many methods based on the restraint of various factors (such as evaporative flux, capillary and Marangoni flow, and interactions between substrate and non-volatile solute) have been described throughout the thesis for wholly controlling evaporative self-assembly to create regular structures. The method implemented in this thesis by controlling Brownian particles making a

random movements is to create a random optical potential field associated with the speckle pattern, which means a generation of a complex interference pattern with the effect of the scattering of coherent light by a random medium. This provided us very useful and ideal solution to study such phenomena.

Optical forces, optical potentials and in particular the speckle patterns mentioned in this thesis are very promising to control self-assembly of colloidal particles and multi-particle organizations. Particles in 2D and 3D can be patterned by creating optical fields and therefore several structures from micro objects can be formed. So, the realization of cubic structures and other crystalline lattices is within the bounds of possibility by creating templates for the nucleation of larger crystals. Moreover, this templating is ranging from colloids to biological cells. So, this makes it possible to perform several studies extending from tissue generation to cell differentiation in cell biology [106].

Drying droplets containing volatile solvent and non-volatile solutes, and so patterned deposition of particles have become a very important study especially in recent years in terms of several applications and usage areas. As shown in this thesis, any droplet consisting of colloid, or colloid and active particle, which is E. Coli cell here, is prone to randomly irregular organized, non-uniform and non-equilibrium structure formation. However; homogeneous surface patterns with a highly ordered spatial arrangement is very important for applications in biotechnology, microelectronics, data storage devices, lithography, high resolution ink-jet printing, medical diagnosis and drug discovery, chromatography, thin films and functional coatings, optoelectronics, DNA and RNA micro-arrays, electronic circuits. Also, thanks to these studies about controlling the ring deposition process, perhaps in the future it would be possible to create small particle tools as new micro-physics tools operating at a scale where current tools cannot manipulate particles.

In order to solve this fascinating problem it is possible to change several physical parameters such as evaporation and surface tension, or many other methods mentioned in Chapter 1 and 4 can be implemented to suppress and even control the coffee-ring effect. Our hypothesis was it can be achieved by also applying

optical potential by creating speckle patterns and as shown in Chapter 5, this thought has been verified.



## REFERENCES

- [1] B. Shl. The mystery about the "coffee ring effect" continues. <http://gizmodo.com/the-mystery-about-the-coffee-ring-effect-continues-1785521172> Accessed December 13, 2016.
- [2] J. Clain. How to get rid of old blood stains on bed mattress? <http://b4tea.blogspot.com.tr/2013/03/how-to-get-rid-of-old-blood-stains-on.html>. \hskip.11em plus. 33em minus-.07em Accessed July 23, 2017
- [3] D. Noguera Marín. Colloidal assembly by convective deposition. the role of electric charge, substrate wettability and particle density. 2016.
- [4] B. Wrang. Primitivo. <http://bjarkewrang.dk/primitivo/> Accessed July 23, 2017.
- [5] S. Maheshwari, L. Zhang, Y. Zhu, and H.-C. Chang. Coupling between precipitation and contact-line dynamics: Multiring stains and stick-slip motion. *Physical review letters*, 100(4):044503, 2008.
- [6] S. Abramchuk, A. Khokhlov, T. Iwataki, H. Oana, and K. Yoshikawa. Direct observation of dna molecules in a convection flow of a drying droplet. *EPL (Europhysics Letters)*, 55(2):294, 2001.
- [7] P. A. Kralchevsky and N. D. Denkov. Capillary forces and structuring in layers of colloid particles. *Current Opinion in Colloid & Interface Science*, 6(4):383–401, 2001.
- [8] M. Layani, R. Berman, and S. Magdassi. Printing holes by a dewetting solution enables formation of a transparent conductive film. *ACS applied materials & interfaces*, 6(21):18668–18672, 2014.
- [9] J. Xu, J. Xia, S. W. Hong, Z. Lin, F. Qiu, and Y. Yang. Self-assembly of gradient concentric rings via solvent evaporation from a capillary bridge. *Physical review letters*, 96(6):066104, 2006.
- [10] V. Lotito and T. Zambelli. Self-assembly and nanosphere lithography for large-area plasmonic patterns on graphene. *Journal of colloid and interface science*, 447:202–210, 2015.

- [11] J. R. Trantum, D. W. Wright, and F. R. Haselton. Biomarker-mediated disruption of coffee-ring formation as a low resource diagnostic indicator. *Langmuir*, 28(4):2187–2193, 2011.
- [12] C. P. Gulka, J. D. Swartz, J. R. Trantum, K. M. Davis, C. M. Peak, A. J. Denton, F. R. Haselton, and D. W. Wright. Coffee rings as low-resource diagnostics: detection of the malaria biomarker plasmodium falciparum histidine-rich protein-ii using a surface-coupled ring of ni (ii) nta gold-plated polystyrene particles. *ACS applied materials & interfaces*, 6(9):6257–6263, 2014.
- [13] L. Cui, J. Zhang, X. Zhang, L. Huang, Z. Wang, Y. Li, H. Gao, S. Zhu, T. Wang, and B. Yang. Suppression of the coffee ring effect by hydrosoluble polymer additives. *ACS applied materials & interfaces*, 4(5):2775–2780, 2012.
- [14] S. Kundu. Curiosity in coffee ring patterns leads to greater efficiency of energy materials. *Forbes Science*, 2017.
- [15] B. Sobac and D. Brutin. Desiccation of a sessile drop of blood: cracks, folds formation and delamination. *Colloids and Surfaces A: Physicochemical and Engineering Aspects*, 448:34–44, 2014.
- [16] D. Brutin, B. Sobac, B. Loquet, and J. Sampaol. Pattern formation in drying drops of blood. *Journal of Fluid Mechanics*, 667:85–95, 2011.
- [17] Y.-F. Li, Y.-J. Sheng, and H.-K. Tsao. Evaporation stains: suppressing the coffee-ring effect by contact angle hysteresis. *Langmuir*, 29(25):7802–7811, 2013.
- [18] Y. Li, Q. Yang, M. Li, and Y. Song. Rate-dependent interface capture beyond the coffee-ring effect. *Scientific reports*, 6, 2016.
- [19] P. J. Yunker, T. Still, M. A. Lohr, and A. Yodh. Suppression of the coffee-ring effect by shape-dependent capillary interactions. *Nature*, 476(7360):308–311, 2011.
- [20] D. Mampallil, J. Reboud, R. Wilson, D. Wylie, D. R. Klug, and J. M. Cooper. Acoustic suppression of the coffee-ring effect. *Soft matter*, 11(36):7207–7213, 2015.
- [21] F. Macera. Physicists undo the 'coffee ring effect'. <https://phys.org/news/2011-08-physicists-undo-coffee-effect.html> Accessed July 26, 2017.
- [22] W. Kohn. An essay on condensed matter physics in the twentieth century. *Reviews of Modern Physics*, 71(2):S59, 1999.

- [23] U. of Oxford. Condensed matter physics. <https://www2.physics.ox.ac.uk/research/condensed-matter-physics> Accessed July 29, 2017.
- [24] D. Winter. States of matter. <http://users.aber.ac.uk/ruw/teach/334/condmat.php> Accessed December 26, 2016.
- [25] J. Schmalian. Lecture notes: Condensed matter theory i (tkm1). [https://www.tkm.kit.edu/downloads/TKM\\_I\\_2011\\_lecture\\_notes.pdf](https://www.tkm.kit.edu/downloads/TKM_I_2011_lecture_notes.pdf) Accessed December 26, 2016.
- [26] C. N. Likos. Effective interactions in soft condensed matter physics. *Physics Reports*, 348(4):267–439.
- [27] E. Nazockdast and J. F. Morris. Microstructural theory and the rheology of concentrated colloidal suspensions. *Journal of Fluid Mechanics*, 713:420–452, 2012.
- [28] K. Sabareesh, S. S. Jena, and B. Tata. Dynamic light scattering studies on photo polymerized and chemically cross-linked polyacrylamide hydrogels. In *AIP Conference Proceedings*, volume 832, pages 307–310. AIP, 2006.
- [29] S. S. Jena, H. M. Joshi, K. Sabareesh, B. Tata, and T. Rao. Dynamics of deinococcus radiodurans under controlled growth conditions. *Biophysical journal*, 91(7):2699–2707, 2006.
- [30] S. K. Velu, M. Yan, K.-P. Tseng, K.-T. Wong, D. M. Bassani, and P. Terech. Spontaneous formation of artificial vesicles in organic media through hydrogen-bonding interactions. *Macromolecules*, 46(4):1591–1598, 2013.
- [31] A. Kostopoulou, S. K. Velu, K. Thangavel, F. Orsini, K. Brintakis, S. Psycharakis, A. Ranella, L. Bordonali, A. Lappas, and A. Lascialfari. Colloidal assemblies of oriented maghemite nanocrystals and their nmr relaxometric properties. *Dalton Transactions*, 43(22):8395–8404, 2014.
- [32] R. J. Hunter. *Foundations of colloid science*. Oxford University Press, 2001.
- [33] S. J. Ebbens and J. R. Howse. In pursuit of propulsion at the nanoscale. *Soft Matter*, 6(4):726–738, 2010.
- [34] R. Wittkowski. Brownian dynamics of active and passive anisotropic colloidal particles. 2012.
- [35] C. Bechinger, R. Di Leonardo, H. Löwen, C. Reichhardt, G. Volpe, and G. Volpe. Active particles in complex and crowded environments. *Reviews of Modern Physics*, 88(4):045006, 2016.

- [36] E. Pınar, S. K. Velu, A. Callegari, P. Elahi, S. Gigan, G. Volpe, and G. Volpe. Disorder-mediated crowd control in an active matter system. *Nature communications*, 7, 2016.
- [37] P. E. Stephen Lower. Colloids and their uses. [http://chem.libretexts.org/Textbook\\_Maps/General\\_Chemistry\\_Textbook\\_Maps/Map%3A\\_Chem1\\_\(Lower\)/07%3A\\_Solids\\_and\\_Liquids/7.11%3A\\_Colloids\\_and\\_their\\_Uses#title](http://chem.libretexts.org/Textbook_Maps/General_Chemistry_Textbook_Maps/Map%3A_Chem1_(Lower)/07%3A_Solids_and_Liquids/7.11%3A_Colloids_and_their_Uses#title). Accessed October 17, 2016.
- [38] S. Clarified. Colloid. <http://www.scienceclarified.com/Ci-Co/Colloid.html> Accessed October 17, 2016.
- [39] Nanotechnology: New name, old science. *Particle Sciences*, 2011.
- [40] ScienceHQ. Properties of colloidal solution. <http://www.sciencehq.com/chemistry/properties-of-colloidal-solution.html> Accessed March 11, 2016.
- [41] Tyndall effect. <http://www.icoachmath.com/chemistry/definition-of-tyndall-effect.html> Accessed October 17, 2016.
- [42] askIITians Engineering Medical Foundation. Properties of colloids. <http://www.askiitians.com/iit-jee-chemistry/physical-chemistry/surface-chemistry/properties-of-colloids.html> Accessed October 17, 2016.
- [43] T. T. FAQ. What is the tyndall effect? <http://www.tech-faq.com/tyndall-effect.html> Accessed March 11, 2016.
- [44] Colloid. *Britannica Academic*, 2016.
- [45] R. Zsigmondy. Colloids and the ultra microscope. *Journal of the American Chemical Society*, 31(8):951–952, 1909.
- [46] TutorVista. Proof of matter from brownian motion. <http://www.tutorvista.com/content/physics/physics-i/matter/brownian-motion.php> Accessed October 17, 2016.
- [47] A. Mourchid, A. Delville, J. Lambard, E. Lecolier, and P. Levitz. Phase diagram of colloidal dispersions of anisotropic charged particles: equilibrium properties, structure, and rheology of laponite suspensions. *Langmuir*, 11(6):1942–1950, 1995.
- [48] U. E. S. of Pharmacy. Properties of colloids. <https://pharmlabs.unc.edu/labs/colloids/properties.htm> Accessed October 17, 2016.
- [49] T. Bigger. What are the applications of colloids? <http://www.thebigger.com/chemistry/surface-chemistry/>

[what-are-the-applications-of-colloids/](#) Accessed October 17, 2016.

- [50] B. Behkam and M. Sitti. Bacterial flagella assisted propulsion of patterned latex particles: Effect of particle size. In *2007 7th IEEE Conference on Nanotechnology (IEEE NANO)*, pages 723–727. IEEE, 2007.
- [51] B. Behkam and M. Sitti. Bacterial flagella-based propulsion and on/off motion control of microscale objects. *Applied Physics Letters*, 90(2):023902, 2007.
- [52] V. Arabagi, B. Behkam, E. Cheung, and M. Sitti. Modeling of stochastic motion of bacteria propelled spherical microbeads. *Journal of Applied Physics*, 109(11):114702, 2011.
- [53] A. Ashkin. Acceleration and trapping of particles by radiation pressure. *Physical review letters*, 24(4):156, 1970.
- [54] G. V. Philip H. Jones, Onofrio M. Marago. *Optical Tweezers-Principles and Applications*. Cambridge, 2016.
- [55] J. E. Molloy and M. J. Padgett. Lights, actions: optical tweezers. *Contemporary Physics*, 43(4):241–258, 2002.
- [56] J. W. Shaevitz. A practical guide to optical trapping. 2006.
- [57] S. M. Block, D. F. Blair, and H. C. Berg. Compliance of bacterial flagella measured with optical tweezers. 1989.
- [58] S. M. Block, L. S. Goldstein, and B. J. Schnapp. Bead movement by single kinesin molecules studied with optical tweezers. 1990.
- [59] S. M. Block, C. L. Asbury, J. W. Shaevitz, and M. J. Lang. Probing the kinesin reaction cycle with a 2d optical force clamp. *Proceedings of the National Academy of Sciences*, 100(5):2351–2356, 2003.
- [60] R. Mallik, B. C. Carter, S. A. Lex, S. J. King, and S. P. Gross. Cytoplasmic dynein functions as a gear in response to load. *Nature*, 427(6975):649–652, 2004.
- [61] D. G. Grier. A revolution in optical manipulation. *Nature*, 424(6950):810–816, 2003.
- [62] A. M. P. Alberto Fernandez-Nieves. *Fluids, Colloids and Soft Materials: An Introduction to Soft Matter Physics*. John Wiley&Sons, 2016.
- [63] K. Camenzind, C. San Ramon, and L. T. Center. Quantifying trapping forces in a simplified optical tweezers setup. 2013.

- [64] A. Radenovic. Optical trapping handout. <http://lben.epfl.ch/files/content/sites/lben/files/users/179705/Optical%20Trapping%20Handout.pdf> Accessed March 11, 2016.
- [65] P. A.Kas. Introduction-optical traps. <https://www.uni-leipzig.de/~pwm/web/?section=introduction&page\unhbox\voidb@x\bgroup\let\unhbox\voidb@x\setbox\@tempboxa\hbox{o\global\mathchardef\accent@spacefactor\spacefactor}\accent9o\egroup\spacefactor\accent@spacefactoropticaltraps> Accessed December 5, 2016.
- [66] R. E. Holmlin, M. Schiavoni, C. Y. Chen, S. P. Smith, M. G. Prentiss, and G. M. Whitesides. Light-driven microfabrication: Assembly of multicomponent, three-dimensional structures by using optical tweezers. *Angewandte Chemie*, 39(19):3503–3506, 2000.
- [67] K. Visscher, S. P. Gross, and S. M. Block. Construction of multiple-beam optical traps with nanometer-resolution position sensing. *IEEE Journal of Selected Topics in Quantum Electronics*, 2(4):1066–1076, 1996.
- [68] H. Zhang and K.-K. Liu. Optical tweezers for single cells. *Journal of The Royal Society Interface*, 5(24):671–690, 2008.
- [69] K. Visscher, G. Brakenhoff, and J. Krol. Micromanipulation by “multiple” optical traps created by a single fast scanning trap integrated with the bilateral confocal scanning laser microscope. *Cytometry*, 14(2):105–114, 1993.
- [70] K. C. Vermeulen, J. van Mameren, G. J. Stienen, E. J. Peterman, G. J. Wuite, and C. F. Schmidt. Calibrating bead displacements in optical tweezers using acousto-optic deflectors. *Review of Scientific Instruments*, 77(1):013704, 2006.
- [71] E. R. Dufresne, G. C. Spalding, M. T. Dearing, S. A. Sheets, and D. G. Grier. Computer-generated holographic optical tweezer arrays. *Review of Scientific Instruments*, 72(3):1810–1816, 2001.
- [72] R. Eriksen, V. Daria, and J. Gluckstad. Fully dynamic multiple-beam optical tweezers. *Optics Express*, 10(14):597–602, 2002.
- [73] G. Volpe, L. Kurz, A. Callegari, G. Volpe, and S. Gigan. Speckle optical tweezers: micromanipulation with random light fields. *Optics express*, 22(15):18159–18167, 2014.
- [74] V. Shvedov, A. V. Rode, Y. V. Izdebskaya, D. Leykam, A. S. Desyatnikov, W. Krolikowski, and Y. S. Kivshar. Laser speckle field as a multiple particle trap. *Journal of Optics*, 12(12):124003, 2010.

- [75] D. Loterie, S. Farahi, I. Papadopoulos, A. Goy, D. Psaltis, and C. Moser. Digital confocal microscopy through a multimode fiber. *Optics express*, 23(18):23845–23858, 2015.
- [76] O. S. Design. Multimode fiber: The good, the bad and the rather ordinary. <http://osd.com.au/multimode-fiber-the-good-the-bad-and-the-rather-ordinary/> Accessed December 4, 2016.
- [77] Quora. Can astronauts urinate while they’re standing in space without getting themselves into too much trouble? <https://www.quora.com/Can-astronauts-urinate-while-theyre-standing-in-space-without-getting-themselves-into-too-much-trouble> Accessed December 5, 2016.
- [78] D. Soltman and V. Subramanian. Inkjet-printed line morphologies and temperature control of the coffee ring effect. *Langmuir*, 24(5):2224–2231, 2008.
- [79] S. Jung, H. J. Hwang, and S. H. Hong. *Drops on Substrates*, pages 199–218. WileyVCH Verlag GmbH & Co. KGaA, 2016.
- [80] P. E. Bruce A. Averil. *Chapter11: Liquids*, pages 1290–1402. Saylor Foundation, 2011.
- [81] Hodnett-AP. Chapter 3 water and the fitness of the environment. <http://hodnett-ap.wikispaces.com/Chapter+3+Water+and+the+Fitness+of+the+environment> Accessed December 6, 2016.
- [82] M. Apel. Water beading on a leaf. [https://en.wikipedia.org/wiki/Surface\\_tension#/media/File\protect\kern+.2222em\relaxDew\\_2.jpg](https://en.wikipedia.org/wiki/Surface_tension#/media/File\protect\kern+.2222em\relaxDew_2.jpg) Accessed December 6, 2016.
- [83] Die oberflächenspannung. [http://www.alm4you.com/physik/physik2/b\\_\\_laden\\_1\\_\\_2\\_\\_3.html](http://www.alm4you.com/physik/physik2/b__laden_1__2__3.html) Accessed December 6, 2016.
- [84] T. Young. An essay on the cohesion of fluids. *Philosophical Transactions of the Royal Society of London*, 95:65–87, 1805.
- [85] L. Makkonen. Young’s equation revisited. *Journal of Physics: Condensed Matter*, 28(13):135001, 2016.
- [86] rame hart. Glossary of surface science terms. <http://www.ramehart.com/glossary.htm> Accessed December 7, 2016.
- [87] S. S. Latthe, C. Terashima, K. Nakata, and A. Fujishima. Superhydrophobic surfaces developed by mimicking hierarchical surface morphology of lotus leaf. *Molecules*, 19(4):4256–4283, 2014.

- [88] D. L.Chandler. Explained: Hydrophobic and hydrophilic. <http://news.mit.edu/2013/hydrophobic-and-hydrophilic-explained-0716> Accessed December 9, 2016.
- [89] M. Qua, J. Hea, and J. Zhangb. Superhydrophobicity, learn from the lotus leaf. 2010.
- [90] M. O. Kokornaczyk, G. Dinelli, I. Marotti, S. Benedettelli, D. Nani, and L. Betti. Self-organized crystallization patterns from evaporating droplets of common wheat grain leakages as a potential tool for quality analysis. *The Scientific World Journal*, 11:1712–1725, 2011.
- [91] Y. Deng, X.-Y. Zhu, T. Kienlen, and A. Guo. Transport at the air/water interface is the reason for rings in protein microarrays. *Journal of the American Chemical Society*, 128(9):2768–2769, 2006.
- [92] P. Takhistov and H.-C. Chang. Complex stain morphologies. *Industrial & engineering chemistry research*, 41(25):6256–6269, 2002.
- [93] R. D. Deegan, O. Bakajin, T. F. Dupont, G. Huber, S. R. Nagel, and T. A. Witten. Contact line deposits in an evaporating drop. *Physical review E*, 62(1):756, 2000.
- [94] R. D. Deegan. Pattern formation in drying drops. *Physical review E*, 61(1):475, 2000.
- [95] J. Zhang, S.-K. Kim, X. Sun, and H. Lee. Ramified fractal-patterns formed by droplet evaporation of a solution containing single-walled carbon nanotubes. *Colloids and Surfaces A: Physicochemical and Engineering Aspects*, 292(2):148–152, 2007.
- [96] A. P. Sommer, M. Ben-Moshe, and S. Magdassi. Size-discriminative self-assembly of nanospheres in evaporating drops. *The Journal of Physical Chemistry B*, 108(1):8–10, 2004.
- [97] R. Bhardwaj, X. Fang, and D. Attinger. Pattern formation during the evaporation of a colloidal nanoliter drop: a numerical and experimental study. *New Journal of Physics*, 11(7):075020, 2009.
- [98] A. P. Sommer. Suffocation of nerve fibers by living nanovesicles: A model simulation-part ii. *Journal of proteome research*, 3(5):1086–1088, 2004.
- [99] V. N. Truskett and K. J. Stebe. Influence of surfactants on an evaporating drop: fluorescence images and particle deposition patterns. *Langmuir*, 19(20):8271–8279, 2003.
- [100] J. Rodríguez-Hernández and C. Drummond. *Polymer Surfaces in Motion: Unconventional Patterning Methods*. Springer, 2015.

- [101] D. Anderson, M. Bolshtyansky, and B. Y. Zel'dovich. Stabilization of the speckle pattern of a multimode fiber undergoing bending. *Optics letters*, 21(11):785–787, 1996.
- [102] S. Devineau, M. Anyfantakis, L. Marichal, L. Kiger, M. Morel, S. Rudiuk, and D. Baigl. Protein adsorption and reorganization on nanoparticles probed by the coffee-ring effect: Application to single point mutation detection. *Journal of the American Chemical Society*, 138(36):11623–11632, 2016.
- [103] K. Sefiane. Patterns from drying drops. *Advances in colloid and interface science*, 206:372–381, 2014.
- [104] A. Crivoi and F. Duan. Elimination of the coffee-ring effect by promoting particle adsorption and long-range interaction. *Langmuir*, 29(39):12067–12074, 2013.
- [105] S. J. Kang, V. Vandadi, J. D. Felske, and H. Masoud. Alternative mechanism for coffee-ring deposition based on active role of free surface. *Physical Review E*, 94(6):063104, 2016.
- [106] T. Čižmár, L. D. Romero, K. Dholakia, and D. Andrews. Multiple optical trapping and binding: new routes to self-assembly. *Journal of Physics B: Atomic, Molecular and Optical Physics*, 43(10):102001, 2010.